Biochimica et Biophysica Acta 1787 (2009) 753–772

Contents lists available at ScienceDirect

Biochimica et Biophysica Acta

journal homepage: www.elsevier.com/locate/bbabio

Review

Crystallisation, structure and function of plant light-harvesting Complex II

Tiago Barros, Werner Kühlbrandt *

Max Plank Institute of Biophysics, Department of Structural Biology, Max-von-Laue-Str. 3, D-60438 Frankfurt am Main, Germany

ARTICLE INFO

Article history:
Received 21 January 2009
Received in revised form 12 March 2009
Accepted 13 March 2009
Available online 25 March 2009

Keywords:
Photosynthesis
Light-harvesting
Non-photochemical quenching
Electron microscopy
Crystallisation
Membrane protein

ABSTRACT

The chlorophyll *a*/*b* light-harvesting complex of photosystem II (LHC-II) collects most of the solar energy in the biosphere. LHC-II is the prototype of a highly conserved family of membrane proteins that fuels plant photosynthesis in the conversion of excitation energy into biologically useful chemical energy. In addition, LHC-II plays an important role in the organisation of the thylakoid membrane, the structure of the photosynthetic apparatus, the regulation of energy flow between the two photosystems, and in the controlled dissipation of excess excitation energy under light stress. Our current understanding of the sophisticated mechanisms behind each of these processes has profited greatly from the progress made over the past two decades in determining the structure of the complex. This review presents the developments and breakthroughs that ultimately lead to the high-resolution structure of LHC-II. Based on an alignment of the remarkably well engineered and highly conserved LHC polypeptide, we propose several key features of the LHC-II structure that are likely to be present in all members of the LHC family. Finally, some recently proposed mechanisms of energy-dependent non-photochemical quenching (NPQ) are examined from a structural perspective.

1. Introduction

The plant light-harvesting complex of photosystem II (LHC-II) is arguably the most abundant membrane protein on Earth. The complex was discovered by Philip Thornber in 1965, then at the Twyford Laboratories Ltd., London, a basic research unit subsidiary of the Arthur Guinness Brewery [1]. Thornber was washing up centrifuge tubes he had used to fractionate plant leaf extracts. He noticed that the detergent he used to dissolve the green pellet produced a clear green solution. Out of curiosity, he examined this solution by polyacrylamide gel electrophoresis, then a new technique, and found that it produced two prominent green bands, which he referred as Complex I and Complex II [2,3]. First it was thought that the bands represented the two photosystems I and II. Later it was discovered that Complex I was photosynthetically active, and indeed corresponded to photosystem I (PS-I), whereas Complex II had no photosynthetic activity. It was subsequently identified as the main light-harvesting complex that served as an antenna for the photosystems, and first referred to as LHC [4].

In the past three decades, evidence has accumulated that the photosynthetic antenna of green plants is itself the site of excess energy dissipation under high-light conditions, in a process that is often referred to as non-photochemical quenching (NPQ). In the centre of recent attention has been the energy-dependent component of NPQ (qE), which has been the subject of numerous, sometimes controversial, studies. These complex protective and regulatory processes involve not only LHC-II and the related minor LHCs but also another member of the Lhc family, known as PsbS. The biochemistry, structure and primary antenna function of LHC-II, as well as its role in NPQ, are the subject of this review.

2. Biochemical and functional characteristics

2.1. The Lhc family

LHC-II is the prototype of a large and abundant class of chloroplast membrane proteins that accounts for roughly 30% of all protein in plant thylakoid membranes, and binds roughly half of the total Chl in chloroplasts [5]. The LHC apoproteins are the product of the *Lhc* gene superfamily, which comprises at least 30 homologous genes in *Arabidopsis* [6]. The family contains not only the three main polypeptide components of the major LHC-II, Lhcb1, Lhcb2 and Lhcb3, but also the so-called "minor" antenna complexes of photosystem II (PS-II), referred to as CP24, CP26 and CP29 [7], which originate from the gene products Lhcb6, Lhcb5 and Lhcb4, respectively [8] (Fig. 1). Other members are the antenna complexes of PS-I, Lhca1, Lhca2, Lhca3 and Lhca4 and the related and more recently found Lhca5 and Lhca6 [6]. More distantly related family members are the photoprotective early light-induced stress-response proteins (ELIPS) [9,10], and the PS-II component PsbS [11,12], which in its mature form shares a sequence identity of only 15% with Lhcb1.

LHC-II is nuclear-encoded [13], and the same goes for all family members. The LHC-II cDNA was first isolated [14] and sequenced [15]

* Corresponding author. Tel.: +49 69 6303 3000; fax: +49 69 6303 3002.
E-mail address: werner.kuehlbrandt@mpibp-frankfurt.mpg.de (W. Kühlbrandt).

0005-2728/$ – see front matter © 2009 Elsevier B.V. All rights reserved.
doi:10.1016/j.bbabio.2009.03.012

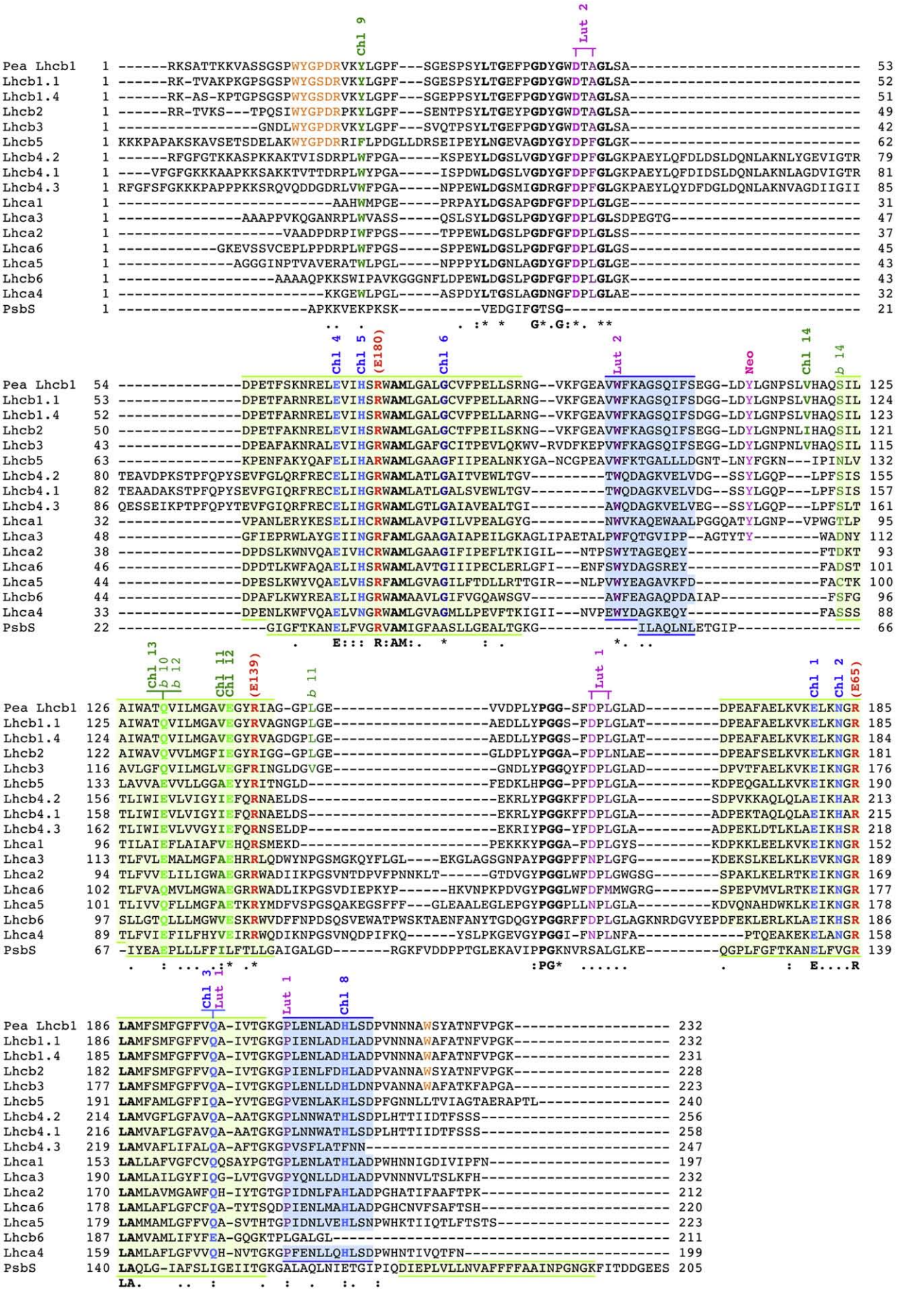
Chl 9
Lut 2
Chl 4
Chl 5
(E180)
Chl 6
Lut 2
Neo
Chl 14
b 14
Chl 13
b 10
b 12
Chl 11
Chl 12
(E139)
b 11
Lut 1
Chl 1
Chl 2
(E65)
Chl 3
Lut 1
Lut 1
Chl 8
Pea Lhcb1
Lhcb1.1
Lhcb1.4
Lhcb2
Lhcb3
Lhcb5
Lhcb4.2
Lhcb4.1
Lhcb4.3
Lhca1
Lhca3
Lhca2
Lhca6
Lhca5
Lhcb6
Lhca4
PsbS

in the early 1980s by Cashmore and co-workers. Members of the LHC-II protein family are distinguished by an extreme degree of sequence conservation, with 58% sequence identity and 77% sequence similarity between Lhcb1, b2 and b3, suggesting that the three-dimensional (3D) structures of three subtypes are virtually identical. The similarity of the mature minor LHCs to Lhcb1 is less pronounced, with sequence identities of 29% for CP24, 45% for CP26 and 32% for CP29, suggesting differences in their 3D structures that may be functionally significant.

LHC-II and its relatives are found only in plants, and are thus a later addition to the arsenal of photosynthetic pigment–protein complexes than the so-called core antenna chlorophyll proteins CP43 and CP47 of PS-II that first arose in cyanobacteria about 3 bn years ago. In contrast to the LHC family, the CP43/47 class of antenna proteins, which also contains the iron stress protein IsiA from marine phytoplankton [16], is encoded by genes in the plant chloroplasts genome [17]. CP43/47 show no obvious sequence or structural similarity to the LHC family [18–20]. In terms of structure and sequence, both classes are different from one another and from the bacteriochlorophyll-containing light-harvesting complexes of the photosynthetic purple bacteria, often referred to as LH1, LH2 and LH3 [21–23].

Not all photosynthetic light-harvesting complexes are membrane proteins. For example, the Bchl *a*-containing "Fenna–Matthews–Olson" complex from the green photosynthetic bacteria *Chlorobium* [24], or the phycocyanins and phycoerythrins of phycobilisomes (reviewed in [25]) are membrane-extrinsic. Antenna complexes are thus much more varied than the photosynthetically active reaction centre complexes, which are always integral membrane proteins. Reaction centres obey the same basic building plan in all photosynthetic organisms, and were thus invented only once. This reflects the fact that light-induced charge separation, the hallmark of photosynthetic reaction centres, requires a special geometry of a pair of Chl or Bchl molecules which ultimately withdraws an electron from a substrate. By contrast, efficient excitation energy transfer in the photosynthetic antenna is clearly possible with many different arrangements of the light-harvesting pigments.

2.2. LHC-II biochemistry

The characteristic dark green colour of the LHC-type antenna complexes is due to their high Chl content, comprising both Chl *a* and Chl *b* in proportions that are, within certain limits, predefined and minimally variable for each complex under native conditions. In addition, the LHCs bind yellow or orange carotenoids, in particular lutein (Lut), neoxanthin (Neo), violaxanthin (Vio), zeaxanthin (Zea) and β-carotene. The three subtypes of the major LHC-II have the same pigment content and spectroscopic properties [26]. Because the LHCs contain comparatively large amounts of Chl *b* (in fact the entire Chl *b* in plants), they have often been referred to as Chl *a*/*b* proteins. By comparison, CP43 and 47 contain only Chl *a*, whereas some of the prochlorophyte members of the IsiA class also contain Chl *b* [27].

The LHC-II apoprotein is synthesized in the cytoplasm and passes through the chloroplast outer and inner envelope, before being inserted into the thylakoid membrane, a process mediated by the chloroplast signal recognition particle [28]. Both cpSRP54 and cpSRP43 are required for membrane targeting [28]. Apparently, the cpSRP recognizes and forms a complex with the DPLG sequence motif at the stromal end of trans-membrane helix 3 that later provides a binding site for Lut 1 [29].

LHC-II and related Chl *a*/*b* binding proteins are able to self-assemble *in vitro*, yielding complexes biochemically and spectroscopically similar to the native complexes isolated from thylakoid membranes. The first LHC-II reconstitution experiments used polypeptides and pigments that were both extracted from thylakoids [30]. A few years later a method was developed to refold LHC-II from isolated pigments and recombinant polypeptide expressed in *E. coli* [31]. Recombinant minor LHCs CP29 [32], CP26 [33] and CP24 [34] were similarly refolded from their components, as were the three different subtypes of LHC-II, Lhcb1, Lhcb2 and Lhcb3 [35], which cannot be isolated in pure form, and the members of the Lhca subfamily [36–38]. With the publication of the first atomic model of LHC-II [39], it became possible to devise and refold mutants that lacked individual Chl binding side chains. In this way, the specific roles of particular pigments in LHC-II could be directly investigated. Soon this strategy was used not only for LHC-II [40,41] but also for the monomeric CP29 [42], and later for Lhca1 [43], Lhca2 [44], Lhca3 [45] and Lhca4 [46]. The capacity of the complex to self-assemble *in vitro* is no less remarkable than its assembly *in vivo*. Based on the dynamics of excitation energy transfer in the process of refolding, it has been suggested that Chl binding during *in vitro* assembly of LHC-II happens in two kinetic phases [47], such that Chl *a* binds predominantly during the first phase, whereas only Chl *b* binds during the second, slow phase [48]. However, the assembly of the mature pigment–protein complex in the membrane, and whether or not it follows the same pathway are not well understood (for a review of recent progress see [49]). Free Chl that is not in van-der-Waals contact with a carotenoid would invariably form triplet states in the light, which in turn would give rise to highly reactive and damaging singlet oxygen. It is therefore thought that Chl must be bound to a molecular chaperone, most likely a protein such as ELIP, in complex with a protective carotenoid before being incorporated into LHC-II.

In the membrane, LHC-II assembles into trimers. The three main subtypes Lhcb1, 2 and 3 seem to combine randomly into trimers of all possible permutations, although they have varying propensities to do so [35]. It has been shown [50] that the WYGPDR motif present in LHC-II and CP26, but not in CP24, CP29 or the Lhca proteins [51] (Fig. 1) is required for trimer formation. The assembly of the LHC-II trimer from monomers most likely occurs spontaneously, as the trimer also assembles readily from monomers in detergent solution [52]. Apparently the monomer–trimer equilibrium is shifted far towards the trimer. Consequently the concentration of free LHC-II monomers in the thylakoid membrane is negligible, whereas the situation is less clear-cut for the minor LHCs. For example, when Lhcb1 and Lhcb2 are absent, trimers of CP26 appear to substitute for the major LHC-II, and the macro-organisation of the PS-II supercomplex is preserved [53].

2.3. LHC-II function

As its name suggests, the primary function of LHC-II is to make the photosynthetic process in green plants more effective by intercepting solar photons and delivering their excitation energy to the reaction centres (Fig. 2). Without such an antenna, the plant photosystems would be hopelessly inefficient. Whereas the PS-II reaction centre contains only 6 chlorophylls (and two pheophytins), it is estimated that there are between 130 and 250 antenna chlorophylls per PS-II core dimer [54], or up to 8 LHC-II trimers ([5]). LHC-II trimers and PS-II reaction centres form supercomplexes of various stoichiometries in the membrane, which can be isolated by mild detergent treatment

Fig. 1. Polypeptide sequence alignment of mature LHCs. All sequences are of *Arabidopsis* genes except the first, which is from pea to highlight key features in the crystal structure [92]. Green background, trans-membrane helix; blue background, amphipathic lumenal helix; orange, N-terminal "trimerisation motif" and C-terminal Trp that are both critical for trimer formation; red, Arg in salt bridges to Glu residues indicated in brackets; black, fully conserved signature residues. Pigment binding residues in the sequence are colour-coded: light blue, Chl *a* side chain ligand; dark blue, Chl *a* backbone ligand *via* water; light green, Chl *b* Mg and formyl side chain ligand; dark green, Chl *b* Mg and formyl backbone ligand *via* water; pink, side chain ligand for carotenoid OH groups; violet, backbone ligand for carotenoid OH groups. (*) indicates strict conservation except for PsbS. Note that Chls 7 and 10 do not have polypeptide ligands but are held in place by coordination of the central Mg to PG and Chl 13 (*via* water), respectively. The program MUSCLE [173] was used for the alignment.

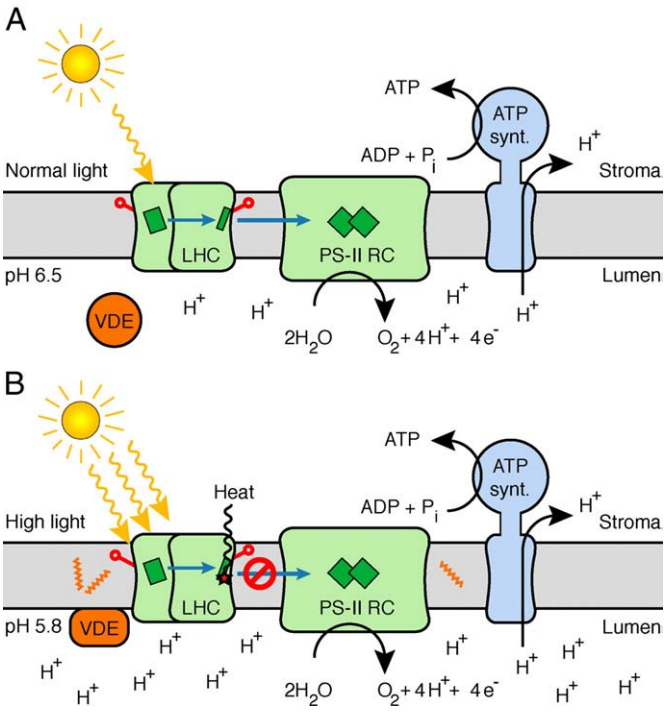

Fig. 2. Light-harvesting and non-photochemical quenching. The LHCs have two important functions in plant photosynthesis. (A) Under normal light conditions, they collect solar energy and transmit it to the reaction centres of the photosystems. (B) Under high-light conditions, the antenna of photosystem II (PS-II) switches to a quenched state, by which photodamage is prevented and excess energy is safely dissipated as heat.

and visualized in the electron microscope [55,56], in which LHC-II trimers and the PS-II dimer can be distinguished. The assignment of other regions to individual minor LHCs is however largely speculative.

The dynamics of light-harvesting and excitation energy transfer within LHC-II have been thoroughly investigated over the years, using a wide variety of spectroscopic techniques (see [57] for review). Apart from their structural and photoprotective roles, the LHC-II carotenoids complement the light-harvesting function of the Chls, thereby increasing the regions of the visible spectrum that can be harvested. The overall carotenoid-to-Chl excitation energy transfer efficiency is estimated to be ~70–90%, with time constants between 50 and 200 ps (see [58] for review). The high-resolution structures, which unambiguously identified the position and identity of all pigments in the complex, greatly assisted the interpretation of the spectroscopic data accumulated at that stage. A model for the excitation energy dynamics has recently been presented [59]. A hallmark of these processes is the efficient and fast energy transfer from Chl *b* to Chl *a*, which typically occurs on the sub-ps time scale. Spatial equilibration of the excitation energy is estimated to be reached within ~48 ps [60], after which it resides predominantly in the Chl *a* cluster comprising Chl 1, Chl 2 and Chl 7 [61] (Table 1). This cluster is situated at the periphery of the trimer, which is the obvious site for efficient energy transfer to photosystems, either directly or *via* the minor LHCs.

More than 30 years ago it was discovered that LHC-II is phosphorylated [62] by a specific kinase [63] at a threonine residue near the N-terminus [64], which is conserved in Lhcb1 and b2, but not in Lhcb3. Phosphorylation of LHC-II enables the plant to adapt to light conditions changing on the timescale of minutes. The main effect of LHC-II phosphorylation appears to be a partial dissociation of the complex from PS-II, and a closer association with PS-I [65]. This is related to state transitions, whereby the antenna funnels more energy into PS-I than into PS-II in state 2, and *vice versa* in state 1 (reviewed by [66–68]). State transitions enable the plant to balance photosynthetic activity between cyclic electron flow around PS-I and vectorial electron flow through PS-II. Consistent with this, the redox state of the plastoquinone pool controls the LHC-II kinase activity, and therefore the state transitions [69]. As Lhcb3 lacks the phosphorylation site, this component, or indeed LHC-II trimers containing it, does not move from PS-II to PS-I, and hence does not participate in state transitions [70].

The LHC-II kinase is required for state transitions and light adaptation [71], proving that LHC-II phosphorylation is the key factor in this process. Accordingly, plants without Lhcb1 and Lhcb2 that lack the phosphorylation site do not undergo state transitions [72]. Mild proteolytic treatment of isolated photosynthetic membranes removes the N-terminal segment of LHC-II on the stromal surface, carrying the phosphorylation site and 3 or 4 Arg and Lys residues, which make it highly positively charged at physiological pH. LHC-II is mainly responsible for membrane appression and grana formation in chloroplast thylakoids. The charged N-terminal segment mediates membrane appression by electrostatic interaction [73]. The electrostatic repulsion between the charged membrane surfaces is reduced by mono- or divalent cations, whereby Mg^{2+} is roughly 10 times more effective than Na^+ or K^+ in charge screening and thus in inducing membrane stacking [74]. *Arabidopsis* mutants lacking both Lhcb1 and Lhcb2 still have chloroplast grana [72], implying that Lhcb3 and other proteins, most likely PS-II, also contribute to grana formation.

3. LHC-II crystallisation

Well-ordered crystals are a prerequisite for determining the precise atomic structure of any protein, and hence for understanding the exact molecular mechanisms and modes of action. Most membrane proteins are notoriously difficult to crystallise, but LHC-II is an exception. Aggregates of two-dimensional (2D) crystals form spontaneously when salt is added to purified, detergent-solubilized LHC-II. Similarly, under the right conditions, small 3D crystals form within seconds, and their growth can be watched in the light microscope (WK, unpublished). Nevertheless it took more than two decades from the first serendipitous observations of crystalline aggregates to the complete, high-resolution structure of the complex.

3.1. Two-dimensional crystals and electron crystallography

The extraordinary propensity of LHC-II for forming crystalline arrays has been noticed from the early days of investigating cation-induced precipitates of the complex in the electron microscope. Freeze-fracture replicas of such *in vitro* aggregates showed that they were stacks of crystalline sheets [75,76], which in some ways resemble stacked thylakoid membranes of chloroplast grana. Crystalline patches of LHC-II were found in negatively stained, reconstituted

Table 1
Chlorophylls nomenclature.

	Standfuss et al. [91]	Kühlbrandt et al. [39]	Liu et al. [89]
Chl *a*			
	Chl 1	*a*1	610
	Chl 2	*a*2	612
	Chl 3	*a*3	613
	Chl 4	*a*4	602
	Chl 5	*a*5	603
	Chl 6	*a*6	604
	Chl 7	*b*2	611
	Chl 8	*b*3	614
Chl *b*			
	Chl 9	–	601
	Chl 10	*a*7	607
	Chl 11	*b*1	608
	Chl 12	*b*5	609
	Chl 13	*b*6	606
	Chl 14	–	605

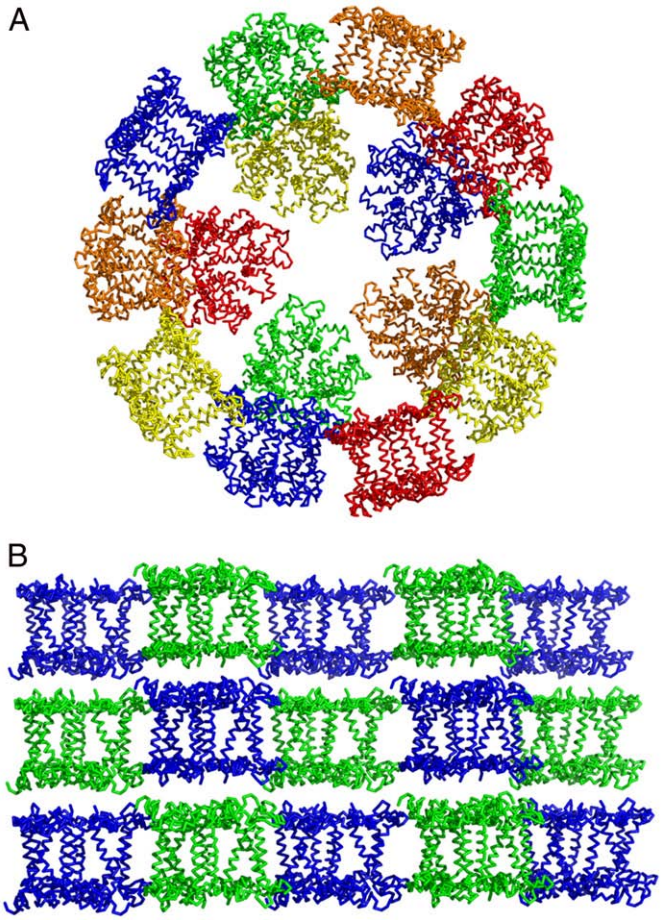

Fig. 3. Three-dimensional crystal packing of LHC-II. The two available high-resolution structures of LHC-II were determined from crystals of two different lattice types. (A) The spinach LHC-II structure was solved from crystals of spherical, icosahedral proteoliposomes, with 20 LHC-II trimers per vesicle [89]. The five trimers facing the viewer were removed for clarity. (B) Type-I crystals consisting of membrane-like two-dimensional crystals yielded the structure of the pea complex [91].

membranes [77]. A systematic investigation of crystalline membranes produced by adding mono- and divalent cations to LHC-II solubilized in Triton X-100 showed that they were two-dimensional crystals of LHC-II trimers alternating in up/down orientation relative to the membrane plane [78]. This arrangement does not exist in native thylakoids, where all complexes naturally face the same way, although the complex does crystallise *in situ* when sufficient detergent is added to membrane preparations to solubilize a proportion of the complexes [79]. The strong tendency to form crystalline membrane arrays is thus a fortuitous property of the complex, quite unrelated to any of its biological functions, evidently for the sole benefit of electron crystallographers and spectroscopists. A first three-dimensional map of such crystalline membranes showed that LHC-II in the 2D crystals is a trimer, and indicated its dimensions and symmetry [80]. Later it was shown by analytical ultracentrifugation that the complex is also a trimer in detergent solution [81].

2D crystallisation conditions were optimised by introducing n-nonyl glucoside (NG) as a second detergent, and by observing a carefully controlled temperature regime. In this way it was possible to avoid stacking and to grow single 2D crystals that measured up to 10 μm across, diffracting electrons to 3.2 Å or better when cooled with liquid nitrogen [82]. At this time, Henderson and colleagues were developing their new method for determining the structures of bacteriorhodopsin by electron diffraction and cryo-EM of 2D crystals at near-atomic resolution [83,84]. The stage was therefore set for using the 2D crystals of LHC-II to work out the structure of this complex by electron diffraction [82], high-resolution cryo-EM and image-processing [39].

3.2. Three-dimensional crystals and X-ray crystallography

Around the time when 2D crystals of LHC-II were first obtained and analyzed, the first reports of diffracting 3D crystals of membrane proteins were published: bacteriorhodopsin [85], bacterial photosynthetic reaction centres [86] and bacterial outer membrane porins [87]. Early attempts to grow 3D crystals of pea LHC-II had in fact been successful and yielded two different crystal forms [88]. One form grew in the shape of octahedra with cubic symmetry and a surprisingly large unit cell. The octahedral crystals were most likely of the same type used later by Liu et al. to determine the 2.7 Å structure spinach LHC-II [89], which consist of icosahedral vesicles of 20 LHC-II trimers (Fig. 3A) packed on a cubic lattice. Indeed, such small vesicles can be seen by negative-stain electron microscopy in preparations of crystalline aggregates (Fig. 4). Most likely, the “heptameric assemblies” of LHC-II reported by Dekker et al. [90] are nothing other than these icosahedral vesicles (Fig. 5) as their appearance and dimensions are identical. Generally, it is not advisable to draw conclusions about the 3D structure of a macromolecular assembly from single view projections.

The other crystal form of LHC-II obtained in the mid-1980s grew in the shape of hexagonal plates. This form evidently consisted of stacked 2D crystals (Fig. 3B), as electron diffraction of thin specimens indicated the same unit cell and apparent symmetry as the 2D arrays [88]. More recently this was confirmed by freeze-fracture electron microscopy of hexagonal crystals, which shows 2D lattices in exact register, forming a 3D lattice (Fig. 6). These crystals were too small for the X-ray sources available at the time, and structure determination by electron crystallography of the well-ordered 2D crystals seemed the more promising alternative. More than 15 years later, the hexagonal plates yielded the 2.5 Å X-ray structure of pea LHC-II [91].

It is interesting to note that the two crystal types of LHC-II are due to two different, fortuitous properties of the LHC-II trimer: one to its unique propensity to form planar 2D lattices in the membrane by surface complementary, and the other to its unrelated ability to form small icosahedral lipid–protein vesicles that resemble virus capsids and pack like spheres into a cubic lattice.

Not every crystal of a membrane protein diffracts well, no matter how perfect it looks to the eye (Fig. 7). Unfortunately in this respect LHC-II is no exception. For the structure of pea LHC-II, more than 400

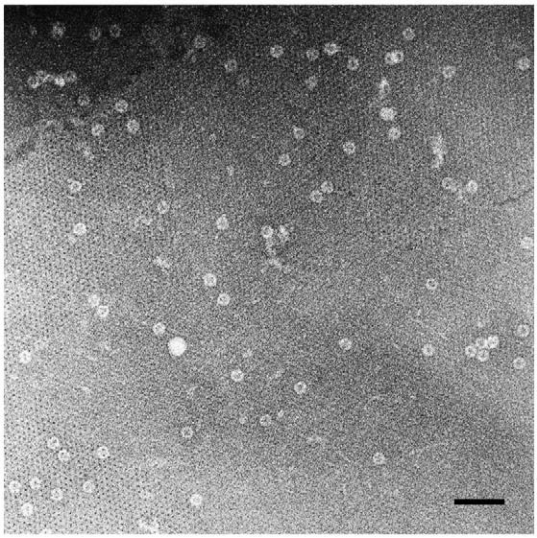

Fig. 4. Icosahedral LHC-II vesicles and stacks of 2D crystals observed by electron microscopy.

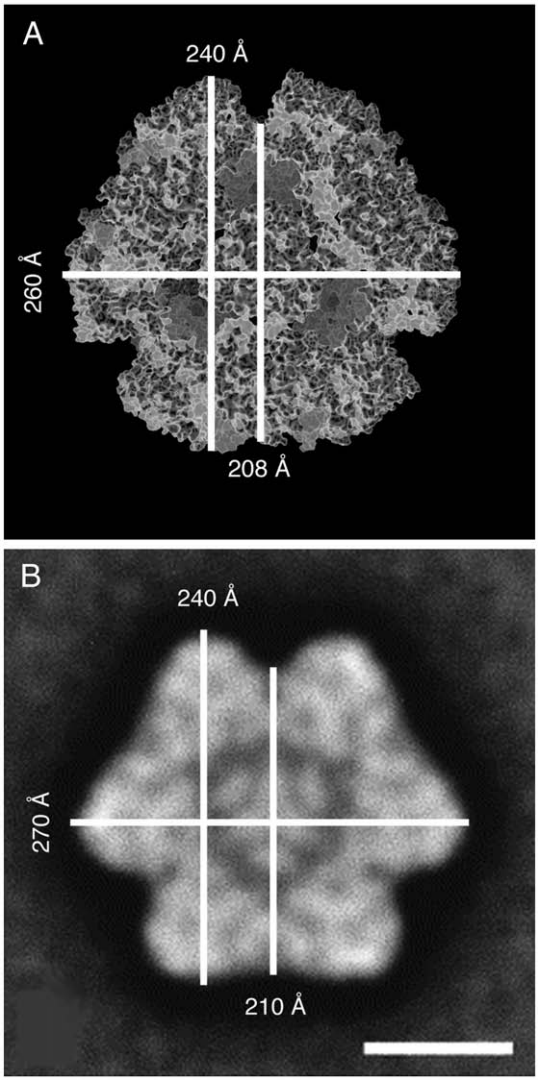

Fig. 5. *In vitro* assemblies of LHC-II. (A) Volume-rendered representation of the 20 trimers in one complete icosahedral vesicle, as in the cubic spinach LHC-II crystals [89]. (B) The dimensions of the LHC-II assemblies described by Dekker et al. [90] are almost identical. Scale bar: 100 nm.

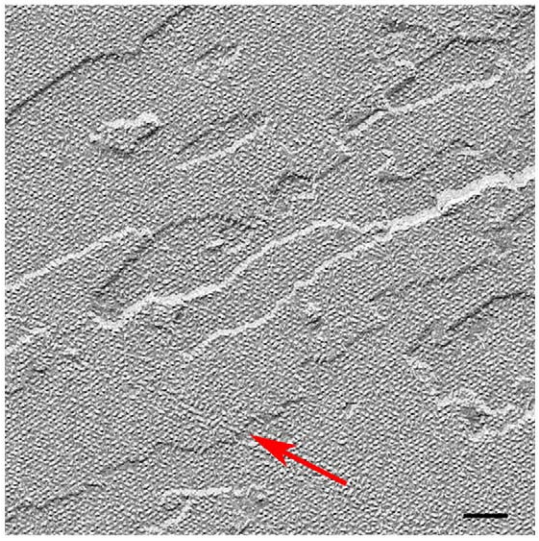

Fig. 6. Freeze-fracture image of a type-I pea LHC-II crystal. Type-I membrane protein crystals [92] are ordered stacks of 2D crystals. Several successive layers can be seen, with all layers in register. Such crystals routinely diffract beyond 3 Å at a synchrotron source. The arrow indicates a crystal defect in one layer, resulting in a displacement of the 2D lattice by about half a unit cell. Scale bar: 100 nm.

individually mounted, rapidly frozen hexagonal crystals had to be examined by X-ray diffraction at the synchrotron before a complete, more or less isotropic data set could be collected. Crystal defects that are not visible in the light microscope are revealed by electron microscopy of freeze-fracture replicas. Consecutive crystalline layers of 2D crystals in type-I lattices [92] can be misaligned (Fig. 8A). The repeat distance between successive layers can vary (Fig. 8B) or protein-free patches may be interspersed (Fig. 8C). Aging crystals may bend almost like rubber (Fig. 8D), although remarkably they still diffracted X-rays in the *x*–*y* plane. The effects shown in Fig. 8B and D would result in resolution anisotropy manifest in poor diffraction in *z*-direction. Most likely similar type-I crystals of other membrane proteins suffer from the same defects.

4. LHC-II structure

4.1. Structures determined by electron microscopy

The first molecular structure of LHC-II determined to 6 Å resolution by electron crystallography showed three alpha helices that span the membrane [93]. The overall dimensions of the kidney-shaped monomer were 30 Å by 50 Å, with a thickness of ~60 Å; the diameter of the roughly cylindrical trimer was ~75 Å. The map showed 15 regions of density that were of the size and shape expected of Chl tetrapyrroles at 6 Å, but no assignment to Chl *a* or *b* was feasible at that early stage. The 6 Å map did however show the close structural similarity between two of the trans-membrane helices and some of the surrounding Chls.

The high-resolution EM structure (PDB code: 2W7B) at 3.4 Å in *x*–*y* direction – and better than 4.9 Å in the perpendicular *z*-direction – made it possible to trace most of the polypeptide chain, especially of the three membrane-spanning helices where bulky side chains were well resolved [39]. 12 Chl tetrapyrroles were identified unambiguously. Apart from the chain trace, the most exciting feature of this map was two elongated regions of density related by the same internal near-twofold symmetry as the two long helices and a subset of the 12 resolved Chls. Based on considerations of symmetry and pigment stoichiometry, these elongated densities were assigned to the two luteins in LHC-II, as it turned out correctly. Even though the structural differences between Chl *a* and *b* were not visible at this resolution, a tentative assignment was made based on the distance of Chls from the two luteins, taking into

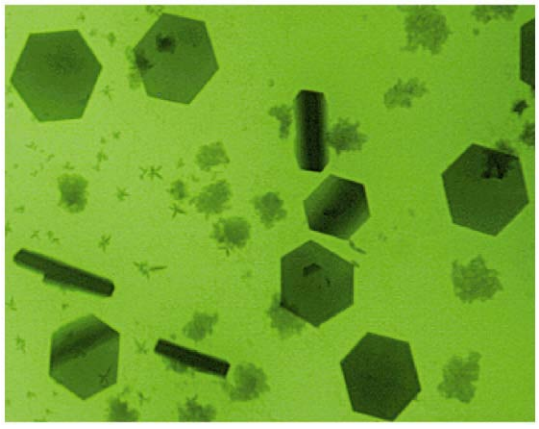

Fig. 7. Hexagonal plates of pea LHC-II.

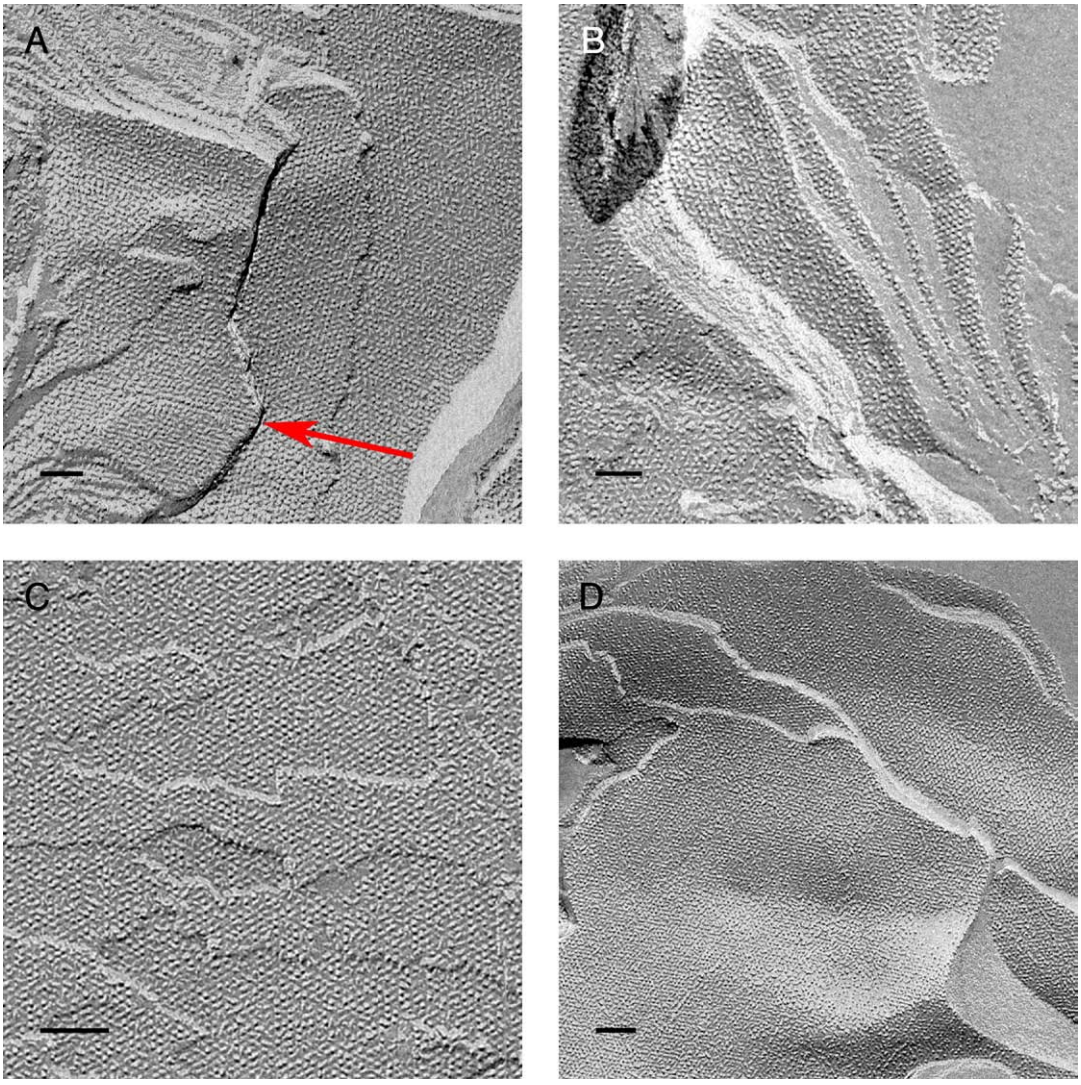

Fig. 8. Defects in the type-I lattice of pea LHC-II crystals. Freeze-fracture shows (A) three rotationally misaligned crystalline layers, (B) different spacing between consecutive layers, (C) small protein-free patches of detergent or lipid. (D) Bent crystalline layers in an aged crystals. The arrow in (A) indicates an in-plane lattice displacement, as in Fig. 6. Scale bar: 100 nm.

account that Chls *a* were more at risk from photodamage than Chls *b*, and therefore needed to be in close contact with carotenoids. This assignment was necessarily incomplete, as the two more peripheral carotenoids were not visible in this map. Nevertheless it proved to be correct for 9 out of the 12 resolved Chls, including the 6 Chls *a* nearest to the two luteins.

4.2. X-ray structures

After the 3.4 Å EM structure, work in our lab was resumed on the hexagonal type-I crystals. This choice was based on the following considerations: a higher-resolution structure of LHC-II was evidently necessary, but the 2D crystals were unlikely to yield such a structure, since they diffracted electrons to better than 3 Å only very occasionally, and could not be improved despite considerable effort. Over the years, the octahedral crystals had yielded diffraction up to 6 Å in our hands, but could not be frozen, which seemed essential for high-resolution data collection. On the other hand we knew the hexagonal crystals to be ordered to at least 3.7 Å from the earlier electron diffraction experiments [88].

The original hexagonal plates had been very small, and it took several years to develop a protocol for growing them to a size where they were both large enough (up to 400 μm across, and 20 μm thick) and well enough ordered for data collection. Still, resolution anisotropy, most likely due to the defects shown in Fig. 6, was a persistent problem that was finally overcome only by screening a large number of crystals.

Work with the hexagonal crystals was progressing well, when the publication of the structure of the spinach complex [89] (PDB code: 1RWT) came as a shock. Evidently, Liu et al. had found ways to improve the octahedral crystals, amongst other things by adding lipid to the crystallisation mix, and were able to freeze them for data collection. The structure was an impressive tour de force in protein crystallography. It confirmed all the features observed in the high-resolution EM map, and revealed additional features that had not been resolved at 3.4 Å, especially the two remaining Chls and the two carotenoids, Neo and Vio.

At this point, we had already solved the structure of the pea complex by X-ray crystallography of the hexagonal plates, ultimately by molecular replacement with the 3.4 Å EM map, and model building and refinement was on the way. The full structure of the pea complex, determined entirely independently of the spinach structure, was finally published in 2005 [91] (PDB code: 2BHW). A detailed comparison of the two structures is presented in Section 4.8. The following sections describe the main features of the LHC-II polypeptide, and of the bound pigments and lipids.

4.3. The LHC-II polypeptide

The chain trace of the LHC-II polypeptide was essentially complete in the 3.4 Å EM structure, apart from an unresolved stretch between helices B and C, which comprises a short amphipathic helix on the lumenal surface, and the first 25 residues at the N-terminus. As had already been obvious from the earlier 6 Å map [93] there were three membrane-spanning helices, two of them (helices 1 and 4 in the X-ray structure; B and A respectively in the EM maps) unusually long and tilted, and related by local near-twofold symmetry (Fig. 9). This symmetrical arrangement reflects an internal repeat in the polypeptide [94] that indicates a gene duplication event in the early evolution of the complex. Many of the more recently reported membrane protein structures show evidence of internal repeats, although in most cases, as e.g. in the aquaporins [95] and Na-coupled solute transporters [96,97] the repeats are inverted, whereas this is not the case in LHC-II. The two long helices are linked by a third, shorter and slightly curved helix (helix 3 in the X-ray structure; C in the EM maps). The two short amphipathic helices on the lumenal side (helices 2 and 5), related by the same local near-twofold symmetry, link helix 1 to helix 3, and helix 4 to the C-terminus.

The two central helices 1 and 4 are interlocked by a symmetrical pair of salt bridges, making this part of the complex particularly rigid. The Arg and Glu residues that form these salt bridges are a signature motif of the family (Fig. 1). The assembly of the two long tilted helices plus the two luteins that sit in the grooves at either side of the helix pair, and the 6 Chls *a* closest to them is the central structural motif of LHC-II and is highly conserved. The interlocking salt bridges are found even in the single-helix ELIPS, which are thus likely to form dimers in the membrane and may be the early ancestors of LHC-II [98]. The residues making this salt bridge are also present in PsbS, which is therefore likely to have the same central coiled-coil helix motif found in LHC-II. Since the glutamate oxygens of both salt bridges each serve as a Chl *a* ligand in LHC-II, PsbS has at least the potential to bind two Chls in these positions. A third salt bridge in helix 3, which provides the Mg ligand for Chl 12, is fully conserved except in PsbS.

It has been shown that a tryptophan (Trp 222 in pea Lhcb1) 11 residues upstream from the C-terminus is critical for trimer formation [99], and that a hydrophobic residue is required in this position for stable trimers. Inspection of the LHC-II structure reveals that Trp 222 is sandwiched between Vio and Chl 10 of the neighbouring trimer, obviously a sensitive site for trimer stability. This finding demonstrates nicely that the presence or absence of a single hydrophobic contact, equivalent to 3 kcal/mol [100], can decide whether or not an oligomeric complex forms in the membrane.

It was suggested early on that membrane appression *in vitro* and thylakoid stacking seen in normal chloroplasts are brought about by the same mechanism and involve LHC-II polypeptides directly [101]. More than 20 years later, the LHC-II structure showed that the positively charged N-terminal segment and the otherwise negatively charged stromal surface of the complex complement one another, and may give rise to a velcro-like interaction between parallel grana membrane surfaces [91]. This would explain why phosphorylation, which effectively neutralizes one positive charge at the N-terminus, reduces this interaction, making it easier for LHC-II to move out of the granal membranes towards PS-I.

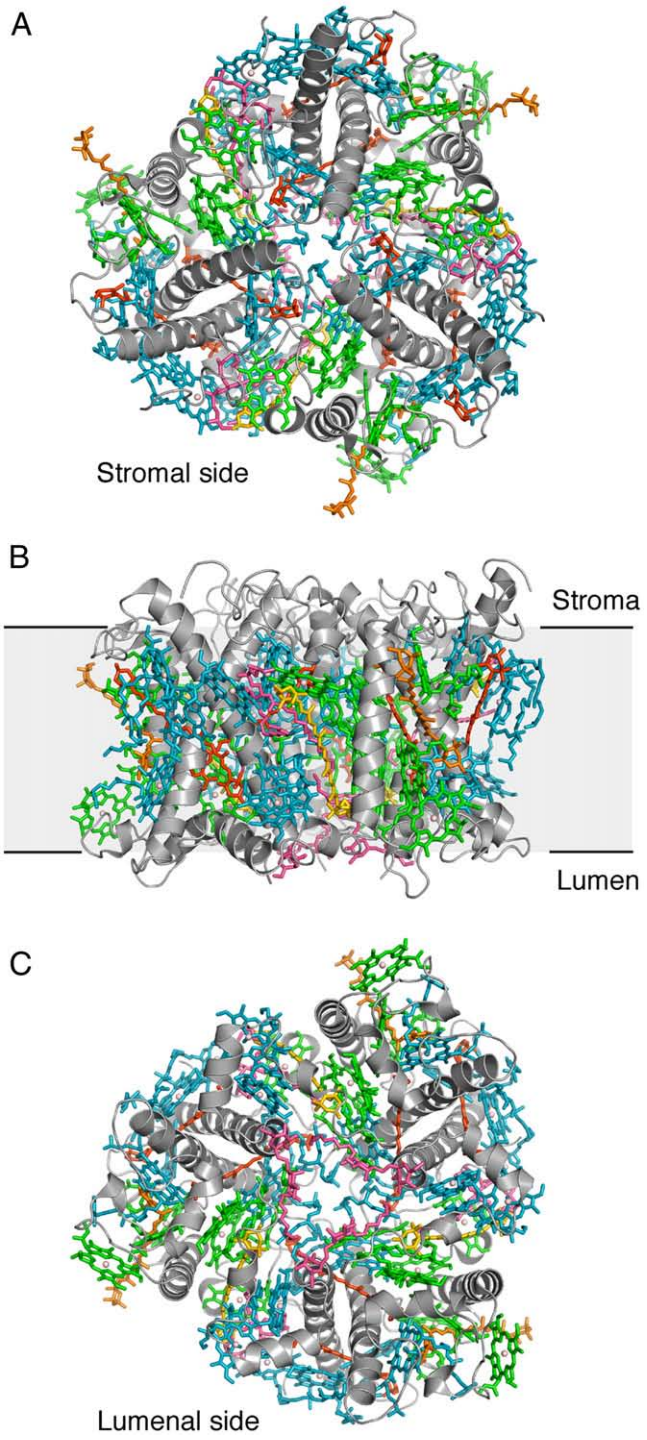

Fig. 9. LHC-II structure. The trimeric complex is shown (A) from the stromal side, (B) from within the membrane and (C) from the lumenal side. Grey, polypeptide; cyan, Chl *a*; green, Chl *b*; dark orange, lutein; light orange, neoxanthin; yellow, violaxanthin; pink, lipids.

4.4. Chl binding sites

The central Mg in the Chl chlorin ring requires an extra ligand with a free electron pair, such as an N or carbonyl O for stable binding. In a protein, these ligands are usually amino acid side chains, or water molecules H-bonded to a main chain carbonyl. Most of the residues involved in Chl binding are conserved throughout the family (Fig. 1). These include the side chains that coordinate Chls 1–5, 8 (except in Lhcb4.3 and 6), 12 and 13, suggesting that these residues bind Chls also in the corresponding family members. Chls 6, 9, 11 and 14 are coordinated by main chain carbonyls *via* a water molecule. The central Mg of Chls 7 and 10 does not have a protein ligand but is coordinated by the PG head group (Chl 7) or a Chl 13 oxygen. For Chls without side chain ligands it is difficult to tell whether their binding sites are conserved or not, although this is likely for Chl 6 which is part of the central set of 6 Chls *a*.

The specificity of a binding site for Chl *a* or *b* is determined by the presence of a hydrogen bonding partner for the Chl *b* formyl group.

Table 2
Pigment composition of native LHC monomers of photosystem II.

LHC	Chl *a*	Chl *b*	Chl *a*/*b*	Lut	Neo	Vio	Chl/Car	Ref.
LHC-II	8	6	1.33	2	1	1	3.5	[89,91]
CP29	6	2	3	1	0.35	0.65	4	[174]
	6.8	2.0	3.4	0.9	0.6	1.2	3.3	[107]
CP26	6.2	2.8	2.2	1.02	0.61	0.38	4.5	[102]
	7.5	3.0	2.5	1.2	1.0	0.9	3.4	[107]
CP24[a] (n)	2.7	2.3	1.17	0.54	–	0.47	5	[34]
CP24[a] (r)	5	5	1	1.5	–	0.5	5	[34]

[a] Values for (n) native and (r) recombinant CP24 are given.

Although Chl *a* sites can be forced to accept Chl *b* and *vice versa* under artificial *in vitro* reconstitution conditions [32,34,102], there is no evidence for mixed occupancy of any Chl site in either X-ray structure. Each binding site therefore seems to be specific for its proper pigment under *in vivo* equilibrium conditions.

In the sequence alignment of Fig. 1, hydrogen bonding donors are fully or partly conserved for the Chl *b* formyls of Chls 10, 11, 12 and 14, so that these are probably also Chl *b* in the corresponding complexes. Chl 7 is likely to be confined to the trimer-forming species, which contain the PG coordinating this pigment. Chl *b* molecules 11 and 14 are most likely present only in the major LHC-II, i.e. Lhcb1-3. A minimum set of Chls common to most LHCs thus includes Chl *a* molecules 1–6 and 8, plus Chl *b* molecules 12 and 13. This is broadly consistent with the experimentally determined Chl content and *a*/*b* ratios of the minor LHCs (Table 2).

4.5. Carotenoid binding sites

Unlike the Chls, carotenoids do not require electron-rich side chain ligands that are easy to spot in a sequence alignment. The LHC-II carotenoids do however have an OH group at each end, and thus the potential to form specific hydrogen bonds to the polypeptide. Close inspection of the LHC-II sequence alignment (Fig. 1) reveals that the binding sites of the lutein head groups in LHC-II are no less highly conserved than the Chl binding sites. The characteristic Lut binding motif is the DPLG sequence in the hook-like extension [93] at the stromal end of trans-membrane helix 4, which is part of the internal repeat and reoccurs in the equivalent extension at the stromal end of helix 1. Whereas in this position the motif has mutated to DTAG in LHC-II, it is repeated without modification in Lhca1, Lhca2 and Lhcb6, which suggests that these proteins are evolutionarily the oldest members of the LHC family. The hook-like shape of this motif provides the stereoselective binding pocket for the Lut head groups, which make two hydrogen bonds each, one to the Asp and the other to the main chain nitrogen before the Gly in this sequence. At the other end of Lut 1 and 2, two highly conserved residues accommodate the other head group and provide a hydrogen bonding partner. Neither of the two lutein-binding DPLG motifs is conserved in PsbS, which is thus unlikely to bind Lut but may bind other carotenoids transiently.

Neo is similarly held in place by a single hydrogen bond between the OH group at its tip and Tyr112, which is conserved in the Lhcbs, except Lhcb6, and an otherwise hydrophobic binding pocket [103]. The high specificity of this binding site for Neo is clearly due to the fact that it can only accommodate the 9′-*cis* stereoisomer (Fig. 14). In WT plants there is no 9′-*cis* carotenoid other than Neo, and virtually all Neo is 9′-*cis* [104,105]. In plant mutants that lack the ability to produce Neo, some of the Vio converts to the 9′-*cis* stereoisomer which can then occupy the Neo site [106]. The Lut and Neo binding sites are thus specific for their respective carotenoid, although they can be forced to accept other carotenoids under non-native conditions, e.g. by *in vitro* refolding or in particular mutants. Vio is the only LHC-II carotenoid that is not held in place by direct polar contacts with the polypeptide scaffold, but by hydrogen bonds of its OH groups to a glycerol OH of PG, and to the phytyl carbonyl of Chl 10. Probably on account of this, and its position at the monomer interface, Vio has a low binding affinity and is easily lost during LHC-II purification [107], presumably as a result of partial dissociation and reassociation of the LHC-II trimer in the presence of detergent.

4.6. Pigment structure

Perhaps the most remarkable property of LHC-II is its ability to bind a total of 54 pigments of 5 different kinds in the small volume of one trimer, and orient them precisely relative to one another. On average, LHC-II uses only 13 amino acids per pigment to achieve this, which makes it almost twice as effective in terms of polypeptide economy compared to bacterial antenna complexes. Within the trimer, the Chls are located in two layers near the stromal and lumenal membrane surface, respectively. Five Chl *a* and three Chl *b* are found in the stromal layer; the other three Chl *a* and three Chl *b* are located in the lumenal layer. The centre-to-centre distances between neighbouring Chls fall within a narrow range of 10 Å to 13 Å. As expected of an efficient solar energy collector, the orientation of the 42 Chl Q_y dipole moments in the trimer sample all directions in space about evenly, maximising light-harvesting efficiency.

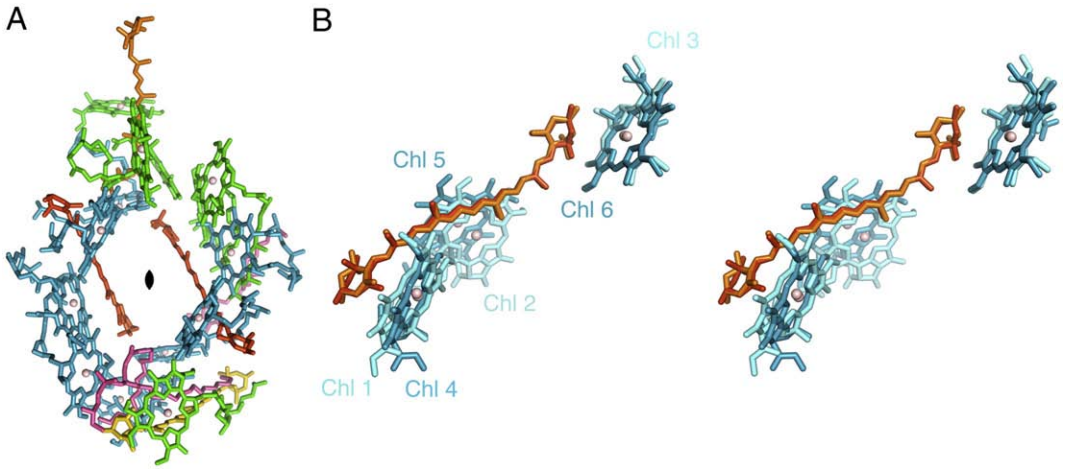

Fig. 10. Pigment configuration in the LHC-II monomer. (A) All pigments bound to one LHC-II monomer are shown, in the same colour code as in Fig. 9. (B) Stereo diagram highlighting the local twofold symmetry of key pigments.

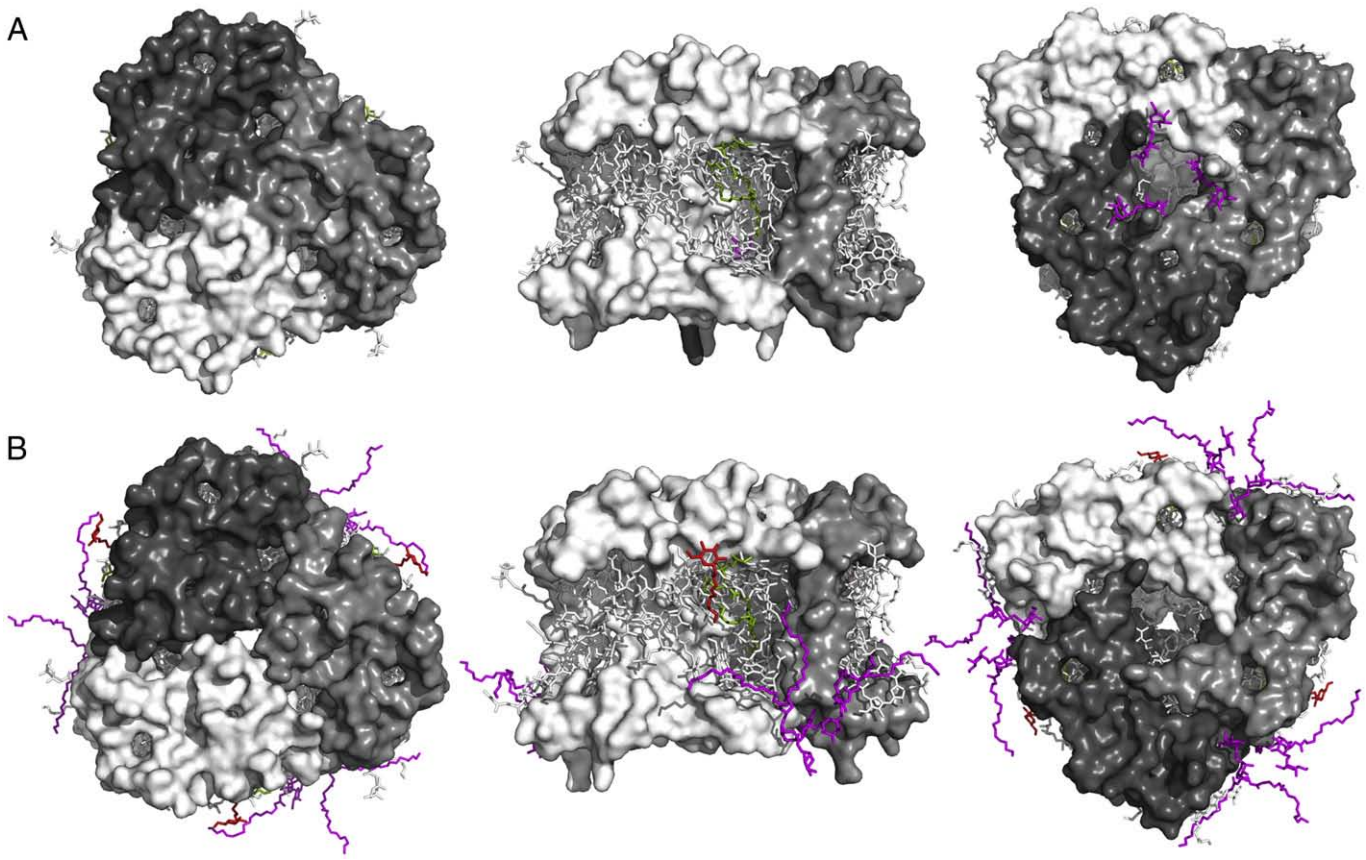

Fig. 11. Lipid and detergent molecules in the LHC-II X-ray structures. The most evident difference between the pea (A) and the spinach (B) LHC-II structure is the location of lipid and detergent molecules. Green, PG; magenta, DGDG; red, NG detergent.

The X-ray structures ended the long-standing uncertainty on the exact number of Chls bound per LHC-II monomer, which is 14 [89,91] (Fig. 9). In retrospect, it is worth noting that precise measurements of the protein concentration of crystalline LHC-II by quantitative amino acid analysis combined with Porra's method of determining Chl *a* and *b* [108] had returned the correct figure of 14.0 Chl per LHC-II monomer in the early 1990s (Nussberger, Dörr and Kühlbrandt, unpublished results). The two high-resolution structures also agreed in the exact position of all 4 carotenoids in the complex.

In the LHC-II trimer, the 6 Chl *b* molecules (Chls 9 to 14) form a cluster around the Neo binding pocket near the monomer interface, suggesting that they may be a later addition compared to the central set of 6 Chls *a* surrounding the luteins. The contact surfaces of Chl 11 and Chl 13 with Neo are especially extensive. Accordingly, a recombinant, refolded LHC-II mutant lacking Chl 13 binds either almost no Neo [109], or only half the amount compared to WT [40,41], depending on the exact refolding conditions. Even so, the complex is still stable and functional, although its ability to form trimers is diminished.

The same local twofold symmetry that relates the two long alpha helices linked by the pair of ion bridges within the LHC-II monomer also applies to the two Luts and the 6 Chls *a* closest to them, and indeed to all Chls in the stromal layer. When superposing the two Luts, Chl 1, Chl 2 and Chl 3 overlap almost perfectly with their symmetry mates Chl 4, Chl 5 and Chl 6 (Fig. 10). This pigment/protein arrangement seems to be an ancient feature that is highly conserved, most likely because it is optimal for light-harvesting, energy transmission and photoprotection. The high conservation of key residues in the LHC fold (Fig. 1) and in the binding pockets of many pigments throughout the LHC family further suggests that this basic arrangement is also shared by the minor LHCs.

In the superposition of Fig. 10, the conformation of the π-system in the two Luts is essentially the same, in contrast to a previous suggestion [110]. Whereas the pair of Lut molecules occupies a central location in the interior of the LHC-II monomer, Vio and Neo assume more peripheral positions. Neo is distinct from the other carotenoids in that roughly half of its length protrudes into the lipid phase of the membrane. As mentioned above, Neo in LHC-II is present almost exclusively as the 9′-*cis* stereoisomer, whereas the other three bound carotenoids are in the all-trans conformation. The significance of this striking feature is still unknown. Its exposed position would make Neo predestined for functionally important interactions with other membrane proteins in the photosynthetic apparatus of green plants. The location of Vio at the monomer-monomer interface would make it easy to exchange this carotenoid for Zea in the xanthophyll cycle [111,112].

Table 3
Superposition of LHC-II X-ray structures.

		rms deviation (Å)	Average (Å)	Maximum (Å)
Polypeptide				
(14 to 231)	Cα	0.35	0.30	2.33
	Main chain	0.40	0.31	3.64
(20 to 220)	Cα	0.34	0.29	1.17
	Main chain	0.35	0.30	1.19
Pigments				
(all Chls)	Mg atoms	0.20	0.18	0.46
	Chlorin rings	0.25	0.23	0.70
Main chain plus pigments				
(14 to 231)	(all Chls)	0.36	0.29	3.64
(20 to 220)	(all Chls)	0.33	0.28	1.21

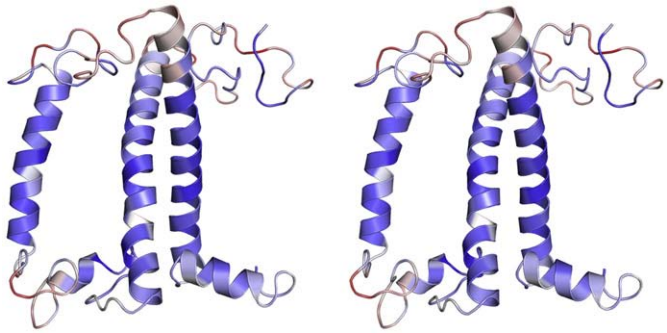

Fig. 12. Stereo diagram showing the rms deviation between pea and spinach LHC-II. The pea LHC-II polypeptide is colour-coded from blue (low rms deviation) through white to red (high rms deviation).

4.7. Bound lipids

In addition to the polypeptide and pigments, two different lipids complete the LHC-II structure. Of these, PG is known to be required for trimer formation [113]. Hydrolysis of PG by phospholipase A2 causes the trimer to break up into monomers, highlighting the structural role of this lipid as a hydrophobic glue between subunits [114]. Dissociation of the trimer into monomers also occurs when the first 49 residues are proteolytically cleaved off the LHC-II polypeptide [114]. This segment includes Tyr44, which makes a polar contact with the PG head group. The segment also includes the upstream WYGPDR "trimerisation motif" common to those LHCs that are known to form trimers *in vivo*; i.e. the major LHC-II itself and CP26. This motif is structurally close to the PG lipid, although no direct contacts are evident. Probably its absence disrupts the PG binding site, so that trimer formation is prevented. PG also coordinates the central Mg of Chl 7, indicating that PG has more than one function in the assembly of the complex.

Like PG, DGDG is required for the formation of both 2D and 3D crystals of LHC-II [114]. While PG is present in one copy per monomer, several molecules of DGDG per monomer co-purify with the trimeric complex. Biochemical experiments had indicated that PG must bind at the monomer interface and has a direct structural role in the trimer, whereas DGDG binds more peripherally [114]. This is indeed borne out by the two high-resolution structures, which show DGDG either in a central hydrophobic cavity on the lumenal side in the higher-resolution structure of the pea complex [91], or at the periphery, bridging the gap between two adjacent trimers on the stromal side of the spinach complex in the highly curved proteolipid vesicles [89] (Fig. 11). In fact, the DGDG position is the most apparent difference between the two LHC-II structures. The lipid in the hydrophobic cavity on the threefold axis is no doubt present in both, but was not resolved by Liu et al. In the structure of the pea complex, DGDG is most likely also present in the large cavities between trimers in the 2D lattice (along with detergent and

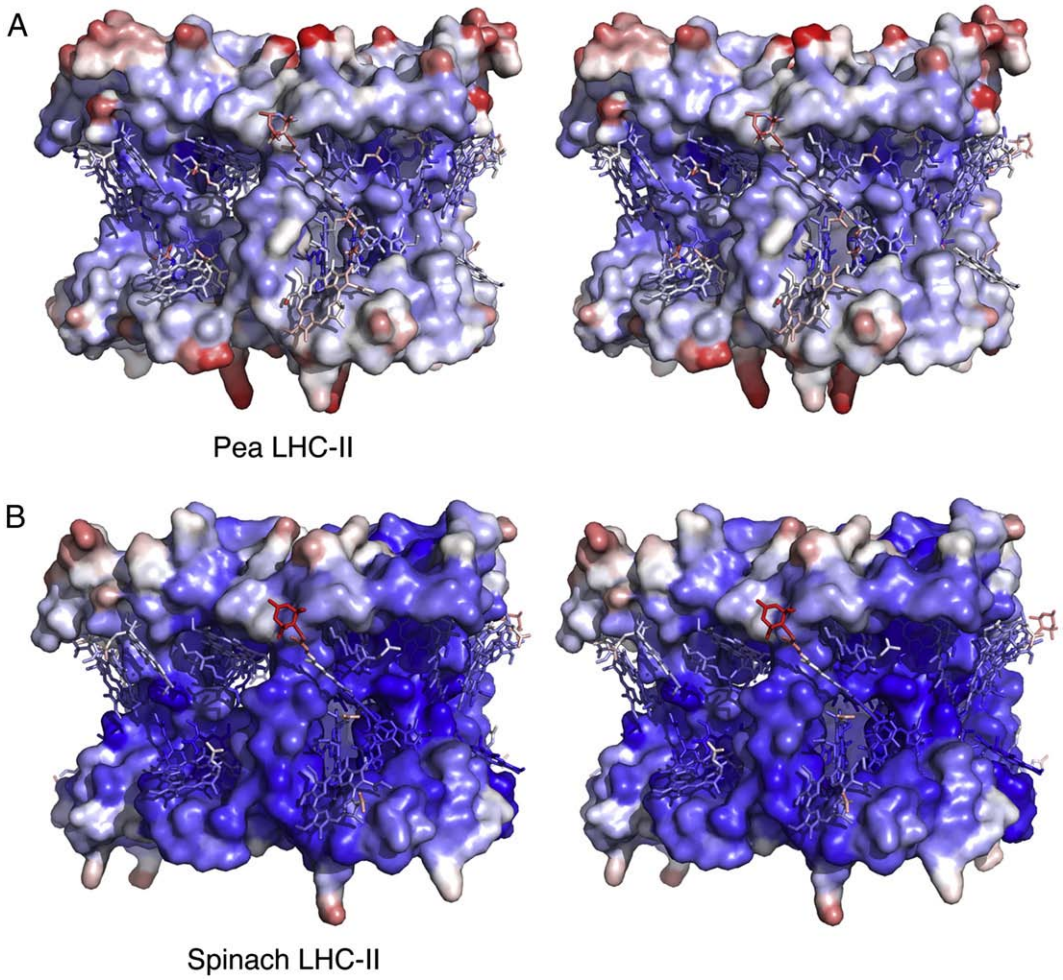

Fig. 13. Stereo diagrams of the B-factor distribution in the structure of (A) pea and (B) spinach LHC-II. The colour gradient goes from blue (lower B-factors, low flexibility) through white to red (higher B-factors, high flexibility). The protein is shown as a solid surface and the pigments in stick representation. Detergent, lipids and phytyl chains are omitted for clarity.

other lipids) but not resolved, as it may not occupy a unique binding site. On the other hand, two ordered molecules of peripherally bound DGDG per monomer are resolved in the structure of the spinach complex, where they mediate contacts between trimers in adjacent trimers forming the icosahedral vesicles, and are thus immobilised. Note however that this particular trimer interaction is not physiological, as it would impose an extreme membrane curvature, which cannot occur in the planar grana thylakoids.

4.8. Comparison of the two X-ray structures

LHC-II is thought by some to undergo a functionally important change of its 3D structure in the process of non-photochemical quenching (see Section 5 below). If the complex is indeed able to adopt different conformations, this should be detectable in the structures of LHC-II from two plant species that are not closely related, determined independently from completely different crystal forms that were grown under different conditions, including pH. A detailed comparison of the two X-ray structure is therefore of interest. In the absence of visible differences between the two structures, the degree of similarity between them will indicate the rigidity or flexibility of the complex, which in turn reflects the likelihood of such a conformational change actually taking place.

The X-ray structures of pea [91] (PDB code: 2BHW) and spinach LHC-II [89] (PDB code: 1RWT) were superposed and compared. Superposition of the main chain polypeptide atoms of residues 14 to 231 that are resolved in both indicates an almost perfect overlap. The rms deviation between all main chain atoms in this range is only 0.40 Å (Table 3). Remarkably, the largest deviation between two equivalent atoms in the main chain between residues 20 and 220 (excluding both termini) of the two structures is less than 1.2 Å.

Fig. 12 shows the rms deviation between the two superposed LHC-II polypeptides. The main structural features of LHC-II, in particular the trans-membrane helices, reveal a high degree of similarity between the two structures. Note that the pigment binding regions are the most similar. The only significant rms deviations are found in the surface loop regions of the polypeptide.

When the atomic coordinates of the pigment are compared, the rms differences are smaller by a factor of almost 2 compared to the polypeptide main chain. This indicates that the pigment structure in LHC-II is even more highly conserved than that of the polypeptide, no doubt because the exact distances and mutual arrangement between Chls on the one hand, and between Chls and carotenoids on the other, are vital for its proper function, which is another reason for assuming that no flexibility of the complex can be allowed.

The polar contacts of the Chl *b* formyl group are also essentially the same in the pea and spinach LHC-II structures, with two exceptions. First, the formyl group of Chl 13 in the spinach structure makes a weak, 3.4 Å polar contact with a nitrogen atom of the Chl 10 tetrapyrrole, whereas the equivalent distance in the pea structure is slightly longer (3.8 Å). While this difference may be simply a question of map interpretation, the other exception cannot be explained so easily. In the spinach crystal structure, the formyl group of Chl 14 makes a polar contact with an acyl group of the DGDG molecule that mediates the inter-trimer contacts in the icosahedral vesicles. In the pea structure this DGDG is absent, and the only hydrogen bond to the Chl 14 formyl group is to the backbone nitrogen of Ser123. As noted above, the location of DGDG in the spinach structure is closely linked to the extreme curvature of the proteoliposome vesicles, so that this polar contact between Chl 14 and DGDG is very unlikely to occur in the membrane. Indeed, it has been suggested that an extra hydrogen bond to a Chl *b* formyl group is present in the cubic crystal form compared to trimers in detergent solution [115], and this evidently is it. The same 1639 cm^{-1} band in the resonance Raman spectrum attributed to the stretching mode of a Chl *b* formyl group had previously been observed in aggregated LHC-II but not in solubilized trimers [116]. This could mean that the icosahedral vesicles are also present in aggregated trimers, and indeed this is the case (Fig. 4).

Apart from the rms deviation between two independently determined experimental structures, another measure of internal flexibility of a protein is the crystallographic temperature factor (B-factor). This parameter is refined against the experimental diffraction data and describes by how much individual atoms, or groups of atoms, oscillate around their mean position in a protein structure. Looking at the X-ray structures of the pea and spinach LHC-II colour-coded for the B-factor (Fig. 13), it is immediately obvious that the distribution is uneven. The surface loops and residues exposed on the stromal and lumenal side of the complex have moderate B-factors and are thus more flexible than the central region of the complex, which is characterised by low B-factors and is hence the most rigid part of the structure. This region comprises the hydrophobic core of the monomer, with its central motif of the coiled helix pair, the two luteins in their binding pockets, the chlorin head groups of all Chls, as well as the third trans-membrane helix. The striking exception in this central region of the complex is the part of the Neo that protrudes by ~9 Å from the trimer surface into the lipid bilayer. When only the carotenoids are considered (Fig. 14), it is clear that the protruding half of Neo stands out by its high temperature factors, whereas the two luteins in the centre of the monomer, and the violaxanthin at the monomer interface have low B-factors. Like the Chl chlorins, they are thus rigid and unlikely to undergo conformational changes. The only light-absorbing part of an LHC-II pigment that has any inherently flexibility is the protruding half of the Neo molecule.

A conformational switch in the central region of LHC-II, which harbours the pigments that have been implicated in NPQ [115,117] seems unlikely for several reasons. This region is packed particularly tightly, which would effectively prevent any movement without disruption of the entire complex, including the opening of the interlocking salt bridges that hold helices 1 and 4 together. Indeed it looks as if the whole interior of LHC-II is designed to prevent such movements, which would make sense in a complex whose proper function depends on the precise distance and alignment of the light-harvesting pigments. A sliding mechanism

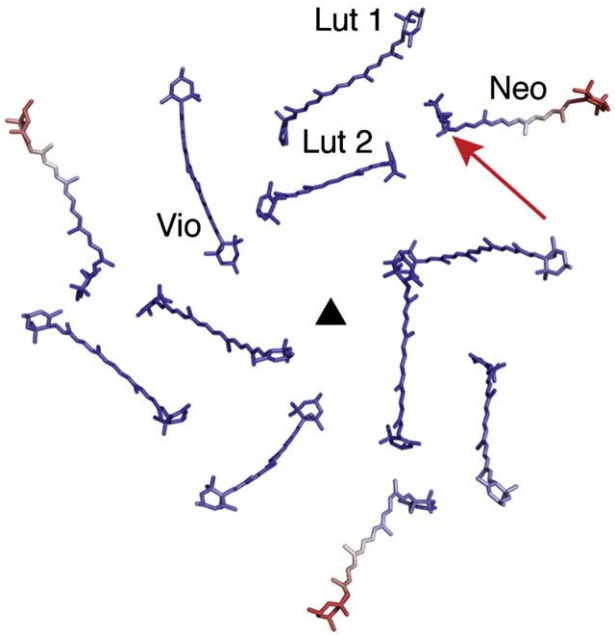

Fig. 14. B-factor distribution in LHC-II carotenoids. The carotenoids in the spinach LHC-II X-ray structure are shown in stick representation and coloured by B-factor as in Fig. 13. Red indicates increasing B-factors and, hence, flexibility. The pigments in one monomer of each trimer are labelled. The triangle indicates the position of the 3-fold symmetry axis in the trimer. Arrow, 9′-*cis* bond in Neo.

by which the distance between Lut and Chls varies gradually in response to photosynthetic activity, as recently proposed [117], can be excluded. Such a movement would only be possible if the corresponding part of the complex is flexible, and this would certainly be reflected in the crystallographic B-factors. Apart from the fact that so far there is no hard, structural evidence for any conformational change in the LHC-II interior, such a switch would be potentially counterproductive and dangerous if it were ever to occur spontaneously [109].

4.9. Conserved structure of plant LHCs

The recent 3.4 Å structure of pea PS-I confirmed that the four Lhca proteins attached to PS-I have the same fold as LHC-II [118]. The characteristic two central, intertwined trans-membrane helices, and the third helix that runs roughly perpendicular to the membrane, superpose almost perfectly with those of LHC-II (Fig. 15A). The only exception is helix 4 (A) of Lhca3, which appears much less tilted and almost parallel to helix 1 (B). In fact, in the superposition of the polypeptide backbones (Fig. 13), this helix of Lhca3 would cut through Lut 2 in the LHC-II structure. As the luteins are amongst the most highly conserved features in the LHC family, and the signature residues that form polar contacts to Lut 1 and 2 are conserved in the Lhca3 sequence (Fig. 1), the apparent orientation of helix 4 in Lhca3 may perhaps reflect the comparatively ill-defined map density in this region.

When the Chl positions are compared in this superposition, it is interesting to note that the arrangement of each Lut in close contact with 3 Chls *a*, as observed in LHC-II, is also found in the Lhcas (Fig. 15B). The only apparent difference is in the orientation of Chl 1 in Lhca1 and Lhca2. This is surprising because Glu180 that coordinates the Chl 1 Mg in the pea structure is strictly conserved in all LHCs and is also involved in the ion bridge with Arg70, which is equally conserved. It might therefore be expected that higher-resolution structures of these complexes will show a closer agreement with the Chl 1 orientation in the other family members. The position of Chl 3 in the 5 structures is remarkably similar. Gln197, which coordinates the Mg of Chl 3 also makes polar contacts to the head group of Lut 1 and to the conserved Asn208. This might explain why the position and orientation of Chl 3 is so similar in LHC-II and the Lhcas. Note that only the polypeptide backbones were used for alignment, so the superposition is not biased by the pigment geometry.

The two prolines at the beginning and end of the short amphipathic helix 5 on the lumenal surface are conserved in most family members except PsbS. In this protein, the predicted, unique fourth trans-membrane helix is supposed to be located in this region, so the lack of sequence conservation is not surprising. The Lhca proteins in the 3.4 Å structure of pea PS-I seem to lack this

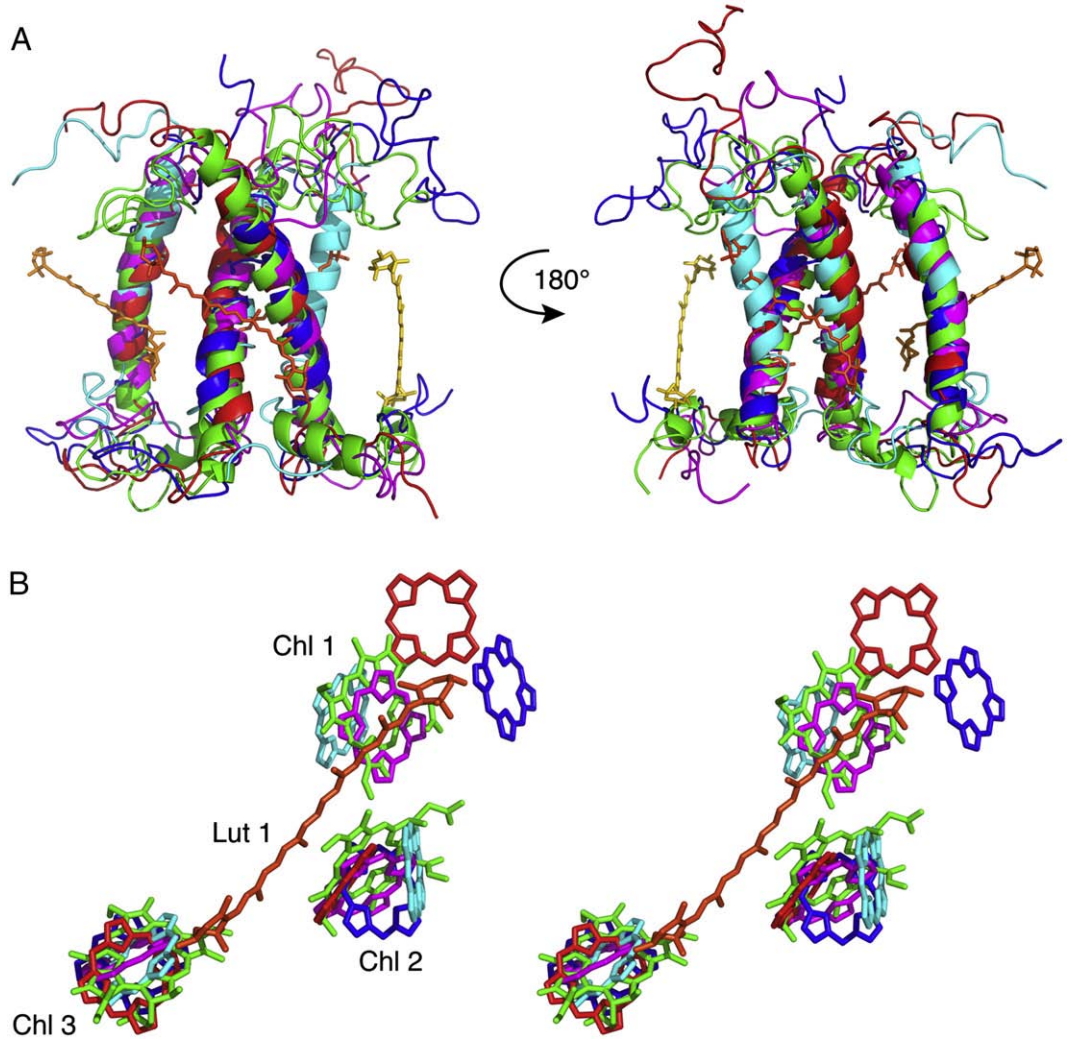

Fig. 15. Comparison of LHC-II and Lhcas. (A) Lhca1, Lhca2 and Lhca4 superpose almost perfectly with LHC-II. One of the central helices of Lhca3 deviates from the others and clashes with Lut 2 in LHC-II. (B) Stereo view of conserved Chl positions in LHC-II and the various forms of Lhca. Differences in chlorin ring orientation may reflect map quality or interpretation. Green, LHC-II; blue Lhca1; red, Lhca2; cyan, Lhca3; magenta, Lhca4; dark orange, Lut; light orange, Neo; yellow, Vio.

amphipathic helix [118], which includes the Chl 8 binding site. The sequence alignment (Fig. 1) indicates clearly that it should be there, suggesting that this helix was perhaps not resolved at 3.4 Å, as was the case for one of the lumenal helices in the 3.4 Å EM structure [39]. The 33 C-terminal residues of PsbS, which have no equivalence in any other LHC, show a striking, but almost certainly coincidental similarity to a sequence in SO4266, a protein of the FIc (Filamentation Induced by cAMP) family from *Shewanella oneidensis* MR-1. The crystal structure of SO4266 (PDB code: 3EQX) reveals that this stretch forms an α-helix [119]. It can therefore be safely assumed that this region of PsbS likewise forms an α-helix, as has been suggested on the basis of its hydrophobicity [120].

5. LHC-II and non-photochemical quenching

Apart from their main light-harvesting function, members of the LHC family also have an essential role in the dissipation of excess solar energy under high-light conditions. The thylakoid membranes of land plants experience frequent and drastic changes in light intensity. Under steady-state conditions, the photosynthetic efficiency of the thylakoid membrane is optimal for a given light level. This level can vary in the time frame of minutes or seconds, be it through changes in cloud cover, or the sudden exposure of a shade leaf to bright sunlight. The resulting potential over-excitation of the photosynthetic system can lead not only to an excessive proton gradient across the thylakoid membrane, but also to photodamage to the photosystems themselves, due to singlet oxygen formation upon interaction of molecular oxygen with Chl triplets. To guard against this, plants have developed a set of photoprotective mechanisms collectively referred to as non-photochemical quenching (NPQ), by which excess excitation energy is safely dissipated as heat.

The assumed, and in some cases well-substantiated roles of plant LHCs in NPQ have been the subject of numerous recent studies and debates. The three components of NPQ, qE, qT, and qI, are each characterised by their relaxation kinetics [121]. Most of the recent investigations have focussed on qE, the rapidly inducible and reversible component of NPQ, which is governed by lumenal pH. Under high-light conditions, protons accumulate in the thylakoid lumen, due to the high activity of the photosynthetic electron transport chain, and the resulting imbalance between proton accumulation in the lumen and the consumption of the proton gradient (ΔpH) for CO_2 fixation and ATP production by the ATP synthase (Fig. 2B). The increase in ΔpH across the thylakoid membrane triggers a series of physiological responses, which ultimately result in qE. The ability to activate qE in coping with a sudden increase in light intensity is crucial for plant fitness in the field [122]. In an effort to identify the main players in qE, it has been shown that *Arabidopsis* plants lacking Lhcb1 and Lhcb2 have reduced qE [72], confirming previous suggestions that LHC-II itself plays an important role in this photoprotective mechanism [123]. However, the exact details of the qE mechanism and the role of LHC-II or the other members of the Lhc family have so far remained elusive.

5.1. Aggregation quenching

The pronounced dependence of the fluorescence properties of LHC-II on its aggregation state has intrigued researchers for more than two decades [124–132]. The bright 680 nm fluorescence and long lifetimes of the detergent-solubilized complex contrast strongly with the quenched fluorescence and very short lifetimes of LHC-II aggregates [125,127,131,132]. Another spectroscopic marker of LHC-II aggregates is the appearance of an emission peak centred around 700 nm at cryogenic temperatures. A drop in Chl fluorescence yield, shorter fluorescence lifetimes at ambient temperature and concomitant increase in 700 nm fluorescence at liquid nitrogen temperature (77 K) was also observed in isolated thylakoids [133,134] or plant leaves [123] under qE conditions. These similarities lead to the aggregation quenching model by Horton [135,136], whereby a pH induced conformational change in LHC-II results in its aggregation in the thylakoid membrane, and ultimately in the enhancement of excitation energy dissipation as heat. This model assumes that (a) LHC-II aggregation occurs *in vivo* and (b) LHC-II can switch between at least two alternative conformations.

We have shown above that some of the larger assemblies presented as evidence of LHC-II aggregation *in vivo*, i.e. the heptameric assemblies of trimers, are in fact proteoliposome vesicles [89], which form from the detergent-solubilized complex. Indirect evidence for LHC-II aggregation *in vivo* comes from spectroscopy, once more based on spectroscopic markers of LHC-II aggregates that were also found in plant leaves [137] and thylakoids [130]. The question is then whether the formation of larger LHC-II assemblies *in vivo*, if it occurs, can generate quenching units, either by internal conformational change or by interactions at the trimer–trimer interface, or whether it just increases the connectivity of the antenna, conducting the excitation energy to another, specifically created quenching unit. van Amerongen and co-workers concluded that *in vitro* aggregation creates energy traps [131]. Holzwarth and co-workers likewise suggested that the quenching mechanism observed with *in vitro* aggregates and NPQ *in vivo* are likely to be the same, involving a Chl–Chl charge-transfer state [137]. Both groups point out that, although the spectroscopic markers of the quenching mechanism *in vitro* and *in vivo* are similar, this does not necessarily mean that the strong interaction of trimers within aggregates also occurs *in vivo*.

Single crystals of LHC-II represent another aggregation state, which is of special interest as the recent X-ray structures of the complex have been determined from them [89,91]. Initial studies lead to the conclusion that the LHC-II in the crystals is quenched, just like aggregates [110,115]. Based on the (incorrect) assumption that there is no energy transfer between the trimers within the crystals, it was further concluded that the corresponding X-ray structure was that of the "crystallisation-induced" quenched conformation of LHC-II. More recently we have demonstrated experimentally that, on the contrary, energy transfer does occur in crystals, with transfer rates similar to those observed *in vivo* [109]. Therefore, the two available X-ray structures show the complex in the fully active, energy transmitting conformation. As no structural evidence for another conformation has been forthcoming, this is presumably the only functional state of the complex. Like others [131,137], we concluded that the *in vitro* quenching interactions between trimers that would be present in aggregates, cannot occur *in vivo*, whereas random quenchers can form at the periphery of the LHC-II trimers. In type-I LHC-II crystals, such quenching centres might form locally due to lattice defects (arrows in Figs. 6 and 8A), which would bring trimers along the line of displacement into close contact, possibly giving rise to such peripheral Chl–Chl pairs.

5.2. The xanthophyll cycle

A well-known consequence of the pH drop in the lumen of the thylakoids is the activation of the xanthophyll cycle [111,112]. In this enzymatic cycle Vio, one of the carotenoids bound to the light-harvesting complex under normal light conditions, is converted to Zea by the lumenal enzyme violaxanthin de-epoxidase. Presumably, the increase in Zea and the concomitant reduction of Vio will result in an exchange of Vio by Zea in the LHCs. Once the light stress is over, the stromal enzyme zeaxanthin epoxidase catalyses the reverse reaction, so that the LHCs return to their initial pigment composition. The xanthophyll cycle and its regulation have recently been reviewed [138].

The effect of the substitution of Vio by Zea on the function of LHC-II is a matter of debate. Some early papers reported quenching induced by Zea [139]. More recently, an 11% reduction in fluorescence quantum

yield upon Zea binding to refolded LHC-II has been reported [140]. Other studies have shown no significant reduction on the Chl excited state lifetimes in Zea-LHC-II [125,141,142]. This is in line with recent calculations, which indicate that the excited state energies of Vio and Zea in LHC-II are virtually identical, and that therefore the simple exchange of xanthophylls is not sufficient for effective dissipation of excess excitation energy [143]. Other effects such as pH-sensing by PsbS are likely to play a role.

Although Zea formation is correlated with qE [144], it is still not clear whether or not Zea binding is necessary for switching the antenna into the quenched state. Some recent studies have conjectured that Zea acts as an allosteric effector of quenching, rather than being directly involved in the quenching mechanism [136,145–149]. In our view this is highly unlikely, given that Zea itself would be an ideal quencher for excited Chls, and is produced in significant quantities during NPQ. If indeed quenching involves Zea bound to an antenna complex, it is then not clear by which mechanism the excitation energy would be dissipated. It could either be excitation energy transfer from Chl to Zea (the gear-shift model; [150]) or through electron transfer from Zea to Chl (the carotenoid radical cation model; [151]). Current opinion leans towards the latter hypothesis. Indeed, the spectroscopic signature of a carotenoid cation radical has been detected in thylakoids under qE conditions [152] but the identity or origin of the radical cation within the photosynthetic apparatus was not identified. Recent experiments have suggested that the minor LHCs, rather than LHC-II itself are the location of the carotenoid radical cation [140,141], although even in this model, Zea binding is thought to be a necessary, but not sufficient step towards quenching [153]. It has been proposed that a conformational change in the minor LHCs is necessary to bring a Chl pair into close contact with a Zea in the L2 binding site, so that they form a quenching charge-transfer state [153]. Although it has been put forward that the Lut 1 site may be occupied by Vio in the minor LHCs (see [49,138] for reviews), this is difficult to prove. L2 is exclusively occupied by Lut in LHC-II, and the high sequence conservation of the Lut binding pockets (Fig. 16) suggests that, on the contrary, *in vivo* both sites are occupied by Lut in all LHCs.

Looking at the structure of the LHC-II monomer (Fig. 16), it is difficult to envisage how carotenoids in the L1 or L2 binding pockets can be exchanged on a fast timescale, without virtually complete disassembly and reassembly of the whole complex. In order to partition from LHC-II into the lipid phase of the membrane, Lut 1 would have to extract itself from behind the tightly bound chlorin ring of Chl 2, while Lut 2 would have to pass the chlorin rings of both Chl 5 and Chl 10, not to mention the phytyl chains of several other Chls. Both replacements would require the breaking of at least 4 hydrogen bonds,

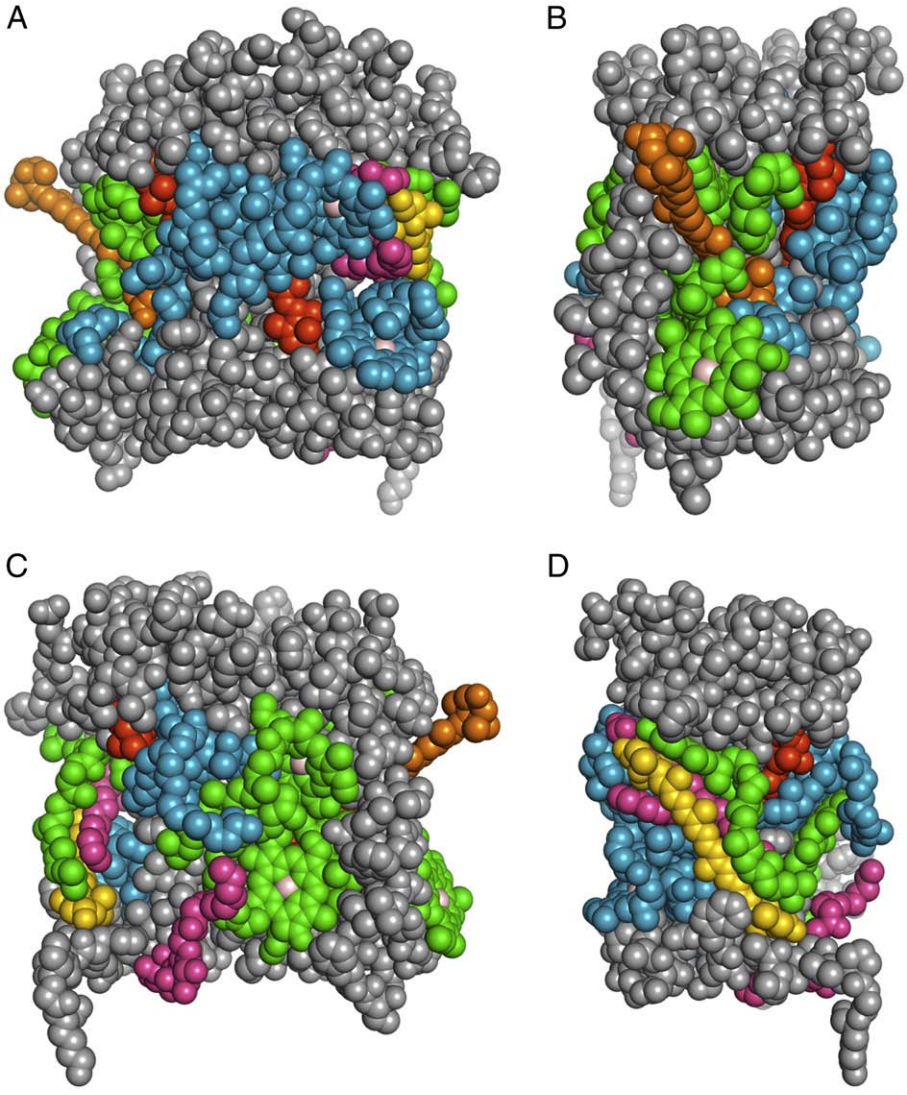

Fig. 16. Accessibility of the L1 and L2 binding sites in the LHC-II monomer shown in four different orientations, rotated by 90° relative to one another. The two luteins (dark orange) are deeply buried in the complex, so that exchange of a carotenoid bound to either site would require disassembly of the complex. Colour coding as in Fig. 9.

which is energetically highly unfavourable in a membrane environment. The binding pockets of Chl 2 and Chl 5 are located in regions of extreme sequence conservation (Fig. 1) that are also the most tightly packed, rigid part of the LHC-II monomer, and the same Chl/carotenoid arrangement is to be expected in the minor LHCs (Fig. 16). When native complexes were used instead to demonstrate Car radical cation formation in the minor LHCs [140], the Zea enriched samples were purified from the *Arabidopsis* npq2 mutant, which lacks both Neo and Vio [154], so that isolated complexes will inevitably have a non-WT pigment composition. For all these reasons, the carotenoid radical cation mechanism for quenching *in vivo* should, for the time being, be regarded as tentative.

5.3. The conformational change hypothesis

The local Chl concentration in LHC-II is roughly 300 mM, yet the complex is able to transmit energy to the reaction centres in the thylakoid membrane, or, in the isolated complex, to re-emit it in the form of fluorescence. By comparison, solutions of free Chl at a similar concentration emit virtually no fluorescence, due to concentration quenching [155], so that all the absorbed light energy is converted into heat. It would therefore only take a small change in the pigment geometry to turn LHC-II from a complex that collects and transmits excitation energy into one that instead dissipates it in the form of heat. It is then tempting to postulate a conformational switch mechanism that would convert LHC-II from an active antenna into a quenching centre under high-light conditions, to protect the photosynthetic apparatus from damage. This conformational change mechanism of LHC-II quenching has been proposed many times [110,115,117,136,147,149,153,156,157].

On the other hand, a highly concentrated and finely balanced system such as LHC-II could easily be quenched by other, spurious effects *in vitro*, such as extrinsic quenching centres close to one of the Chls exposed on the outside of the complex. It would be difficult to differentiate between these two possibilities by spectroscopy. Solid structural studies would be essential to demonstrate a conformational change beyond doubt. So far, no such evidence has been forthcoming.

The observation of two main LHC-II populations with different fluorescence lifetimes in detergent solution was taken as evidence for two conformations (quenched or unquenched) that were supposed to be in equilibrium [156,158]. A variety of experimental procedures have been used to shift this equilibrium towards the quenched conformation: incorporation into liposomes [156], high pressure [158], detergent removal from gel-immobilised complexes [159] and precipitation [117,131]. Evidently, detergent removal or precipitation results in quenched aggregates. Aggregates are also a likely side product when LHC-II is reconstituted into liposomes. Finally, under extreme pressure, non-physiological contacts between LHC-II trimers that form quenching centres are likely to occur. The observed differences between the two alleged conformations were attributed to changes in the Neo conformation and an additional hydrogen bond of the formyl group of at least one Chl *b*. Although Neo is not required for quenching, a change in its conformational has been correlated with the extent of qE *in vivo* [117]. However, as shown here and elsewhere [160], both effects can be explained by parts of pigments exposed on the exterior surface of the complex, i.e. Neo and Chl 14, and thus do not signify an internal rearrangement of the complex.

5.4. Interaction with PsbS

Random mutagenesis studies of *Arabidopsis* lead to the discovery that PsbS is required for qE [161]. In some ways this was a surprise, as quenching by PsbS was thought to require pigment binding, and the protein had already by that time been shown to be stable without bound pigments [162]. Pigment binding by PsbS is still a matter of controversy [163,164]. Two scenarios are possible. Either PsbS participates directly in the quenching event, and in this case it must bind pigments, even if transiently, or it is an effector of qE by interaction with one or several of the LHCs.

A sensitivity of PsbS to the lumenal pH is well-established [165], conferred by two pH-sensing glutamate residues [166] (Glu62 and Glu166 according to the predicted sequence of the mature protein [6] and in Fig. 1). Low pH results in the formation of PsbS monomers [165]. Interestingly, when thylakoids were incubated at low pH, PsbS monomers were predominantly found together with LHC-II, while dimers were preferentially associated with the PS-II core [165]. Two additional lines of evidence support PsbS interaction with the LHCs. First, immunoaffinity experiments have indicated contacts between PsbS and both LHC-II and CP29 [167]. Second, resonance Raman measurements *in vivo* under qE conditions have correlated the distortion of Neo configuration with the PsbS content of the thylakoid membrane [117].

An alternative model of the qE mechanism that reconciles all these considerations and does not require a conformational switch within the LHC is to propose that the PsbS monomers transiently bind pigments under qE conditions, so that by bringing its pigment(s) in close proximity to the LHCs a quenching unit is created [109,168].

6. Conclusion

LHC-II was one of the first membrane proteins to have its structure determined – after the bacterial reaction centre [169], bacteriorhodopsin [170] and bacterial porins [171,172] – and the very first one of eukaryotic origin. In this sense the LHC-II structure heralds a new era, as structural biology of eukaryotic membrane proteins will be a main challenge for the future. Unlike most of the few eukaryotic membrane proteins in the PDB today, LHC-II does not have a bacterial homologue. This will be increasingly the case for other eukaryotic membrane proteins, so in order to find out their molecular structure and mechanisms of these proteins, one has to either isolate these proteins from the cells or tissues where they are abundant, which for LHC-II was easy, because there is so much of it and this is why it came first. But nearly all the naturally abundant eukaryotic membrane proteins have been done (Ca-ATPase, Na/K-ATPase, acetyl choline receptor, aquaporins, VDAC), so in future new proteins will have to be expressed in heterologous or cell-free systems, which is difficult, especially if, as is the case with LHC-II, they form macromolecular assemblies, as many of them do. The functional oligomer of LHC-II was the first eukaryotic membrane protein assembly to be refolded *in vitro* from its components. Again these were pioneering studies that will lead the way to other, even more complex systems.

It seems that almost every single residue in the tightly engineered polypeptide of LHC-II has a special role, from the highly charged N-terminus that controls membrane organisation and grana formation, to the Trp near the C-terminus, which is needed for trimer formation. Probably this is true of most proteins, but rarely is it so visible, because of the numerous, deeply coloured cofactors bound by LHC-II, and the many different pigment or lipid interaction sites.

Today, thanks to a number of important advances in the past decade in determining the structures of the constituent large membrane protein complexes, the photosynthetic membranes of prokaryotes and plants are, along with the mitochondrial respiratory chain, the best-understood membrane system of all. Still, 5 years after the X-ray structure, and 15 years after the 3.4 Å EM structure, LHC-II has not yet yielded all its secrets. In spite of much excellent work, and a good deal of speculation, the mechanisms by which plants protect their photosynthetic system against photodamage are still not well understood.

A long-held hypothesis for NPQ claims that LHC-II itself acts as a molecular switch by changing its internal pigment organisation from a light-harvesting and energy transmitting state to one that instead dissipates the excess energy as heat. However, there never has been

any hard, structural evidence for such change, and indeed, as pointed out in this review and elsewhere [109], such an unprecedented change could easily become counterproductive or even disastrous for a complex whose proper function relies on a precisely optimised, highly conserved pigment geometry. Until such evidence is produced, the conformational change hypothesis will remain just that, an unproven hypothesis. All observations that have been brought forward in support of it can be explained in other, more plausible ways. Most of them are to do with the remarkable tendency of LHC-II to form quenched aggregates under unphysiological conditions *in vitro*, and a certain preference amongst spectroscopists to focus on the properties of these aggregates, which are fascinating in themselves, and easy to prepare and study.

There is however no reason to believe that a sophisticated protective mechanism essential for plant fitness and survival should be left to a single protein. This seems especially unlikely if the protein in question already performs another essential function, which is the exact opposite of dissipating excess energy. In fact this would be unprecedented, if one considers other, similar mechanisms such as the state transitions, which work by changing interactions between different proteins with one another in the membrane. The same is true of signal transmission cascades, chemotaxis, and many other such response mechanisms, and this is likely to be the case also for NPQ.

To finally answer the question "how does non-photochemical quenching work?" will thus require further rigorous experimentation that takes careful account of what the LHC-II structure tells us, combined with advanced biochemistry and yet more detailed spectroscopic studies. More structural studies will be needed, especially of the minor LHCs. These will be more difficult, because the proteins are far less abundant and much less stable than the major antenna complex itself. However, structural biology and protein crystallography are advancing continually, so there is hope that detailed structural information on at least some of the minor LHCs will become available in the future. Also a structure of PsbS, with or without bound pigments, would be extremely interesting and valuable for understanding NPQ, and thus for resolving one of the few remaining fundamental questions in photosynthesis research.

Acknowledgements

We thank Winfried Haase for the freeze-fracture images and Matteo Lamborghini for the photograph of LHC-II crystals. WK acknowledges long-term financial support from SFB 472, which has contributed greatly to five publications [26,35,91,109,141] discussed in this review. TB is supported by the fellowship SFRH/BD/21440/2005 from Fundação para a Ciência e a Tecnologia.

References

[1] J.P. Thornber, Thirty years of fun with antenna pigment-proteins and photochemical reaction centers: a tribute to the people who have influenced my career, Photosynth. Res. 44 (1995) 3–22.
[2] T. Ogawa, F. Obata, K. Shibata, Two pigment proteins in spinach chloroplasts, Biochim. Biophys. Acta 112 (1966) 223–234.
[3] J.P. Thornber, R.P. Gregory, C.A. Smith, J.L. Bailey, Studies on the nature of the chloroplast lamella. I. Preparation and some properties of two chlorophyll–protein complexes, Biochemistry 6 (1967) 391–396.
[4] J.P. Thornber, H.R. Highkin, Composition of the photosynthetic apparatus of normal barley leaves and a mutant lacking chlorophyll b, Eur. J. Biochem. 41 (1974) 109–116.
[5] G.F. Peter, J.P. Thornber, Biochemical composition and organization of higher plant photosystem II light-harvesting pigment-proteins, J. Biol. Chem. 266 (1991) 16745–16754.
[6] S. Jansson, A guide to the *Lhc* genes and their relatives in *Arabidopsis*, Trends Plant Sci. 4 (1999) 236–240.
[7] E.L. Camm, B.R. Green, How the chlorophyll–proteins got their names, Photosynth Res. 80 (2004) 189–196.
[8] S. Jansson, E. Pichersky, R. Bassi, B. Green, M. Ikeuchi, A. Melis, D. Simpson, M. Spangfort, L. Staehelin, J. Thornber, A nomenclature for the genes encoding the chlorophyll *a*/*b*-binding proteins of higher plants, Plant Mol. Biol. Reporter 10 (1992) 242–253.
[9] G. Meyer, K. Kloppstech, A rapidly light-induced chloroplast protein with a high turnover coded for by pea nuclear DNA, Eur. J. Biochem. 138 (1984) 201–207.
[10] I. Adamska, ELIPs — light-induced stress proteins, Physiologia. Plantarum. 100 (1997) 794–805.
[11] N. Wedel, R. Klein, U. Ljungberg, B. Andersson, R.G. Herrmann, The single-copy gene psbS codes for a phylogenetically intriguing 22 kDa polypeptide of photosystem II, FEBS Lett. 314 (1992) 61–66.
[12] S. Kim, P. Sandusky, N.R. Bowlby, R. Aebersold, B.R. Green, S. Vlahakis, C.F. Yocum, E. Pichersky, Characterization of a spinach psbS cDNA encoding the 22 kDa protein of photosystem II, FEBS Lett. 314 (1992) 67–71.
[13] S.D. Kung, J.P. Thornber, S.G. Wildman, Nuclear DNA codes for the photosystem II chlorophyll–protein of chloroplast membranes, FEBS Lett. 24 (1972) 185–188.
[14] R. Broglie, G. Bellemare, S.G. Bartlett, N.H. Chua, A.R. Cashmore, Cloned DNA sequences complementary to mRNAs encoding precursors to the small subunit of ribulose-1,5-bisphosphate carboxylase and a chlorophyll *a*/*b* binding polypeptide, Proc. Natl. Acad. Sci. U. S. A. 78 (1981) 7304–7308.
[15] G. Coruzzi, R. Broglie, A. Cashmore, N.H. Chua, Nucleotide sequences of two pea cDNA clones encoding the small subunit of ribulose 1,5-bisphosphate carboxylase and the major chlorophyll *a*/*b*-binding thylakoid polypeptide, J. Biol. Chem. 258 (1983) 1399–1402.
[16] N.A. Straus, Iron deprivation: physiology and gene regulation, in: D.A. Bryant (Ed.), The Molecular Biology of Cyanobacteria, Kluwer Academic Publishers, 1994, pp. 731–750.
[17] T. Bricker, The structure and function of CPa-1 and CPa-2 in photosystem II, Photosynth. Res. 24 (1990) 1–13.
[18] B. Loll, J. Kern, W. Saenger, A. Zouni, J. Biesiadka, Towards complete cofactor arrangement in the 3.0 Å resolution structure of photosystem II, Nature 438 (2005) 1040–1044.
[19] K.N. Ferreira, T.M. Iverson, K. Maghlaoui, J. Barber, S. Iwata, Architecture of the photosynthetic oxygen-evolving center, Science 303 (2004) 1831–1838.
[20] J.W. Murray, J. Duncan, J. Barber, CP43-like chlorophyll binding proteins: structural and evolutionary implications, Trends Plant Sci. 11 (2006) 152–158.
[21] G. McDermott, S.M. Prince, A.A. Freer, A.M. Hawthornthwaite-Lawless, M.Z. Papiz, R.J. Cogdell, N.W. Isaacs, Crystal structure of an integral membrane light-harvesting complex from photosynthetic bacteria, Nature 374 (1995) 517–521.
[22] R.J. Cogdell, A. Gall, J. Kohler, The architecture and function of the light-harvesting apparatus of purple bacteria: from single molecules to in vivo membranes, Q. Rev. Biophys. 39 (2006) 227–324.
[23] R.A. Brunisholz, H. Zuber, Structure, function and organization of antenna polypeptides and antenna complexes from the three families of Rhodospirillaneae, J. Photochem. Photobiol. B. 15 (1992) 113–140.
[24] R.E. Fenna, B.W. Matthews, Chlorophyll arrangement in a bacteriochlorophyll protein from *Chlorobium limicola*, Nature 258 (1975) 573–577.
[25] W.A. Samsonoff, R. MacColl, Biliproteins and phycobilisomes from cyanobacteria and red algae at the extremes of habitat, Arch. Microbiol. 176 (2001) 400–405.
[26] M.A. Palacios, J. Standfuss, M. Vengris, B.F. van Oort, I.H. van Stokkum, W. Kühlbrandt, H. van Amerongen, R. van Grondelle, A comparison of the three isoforms of the light-harvesting complex II using transient absorption and time-resolved fluorescence measurements, Photosynth. Res. (2006).
[27] J. La Roche, G.W. van der Staay, F. Partensky, A. Ducret, R. Aebersold, R. Li, S.S. Golden, R.G. Hiller, P.M. Wrench, A.W. Larkum, B.R. Green, Independent evolution of the prochlorophyte and green plant chlorophyll *a*/*b* light-harvesting proteins, Proc. Natl. Acad. Sci. U. S. A. 93 (1996) 15244–15248.
[28] D. Schuenemann, S. Gupta, F. Persello-Cartieaux, V.I. Klimyuk, J.D. Jones, L. Nussaume, N.E. Hoffman, A novel signal recognition particle targets light-harvesting proteins to the thylakoid membranes, Proc. Natl. Acad. Sci. U. S. A. 95 (1998) 10312–10316.
[29] K.F. Stengel, I. Holdermann, P. Cain, C. Robinson, K. Wild, I. Sinning, Structural basis for specific substrate recognition by the chloroplast signal recognition particle protein cpSRP43, Science 321 (2008) 253–256.
[30] F.G. Plumley, G.W. Schmidt, Reconstitution of chlorophyll *a*/*b* light-harvesting complexes: xanthophyll-dependent assembly and energy transfer, Proc. Natl. Acad. Sci. U. S. A. 84 (1987) 146–150.
[31] H. Paulsen, U. Rümler, W. Rüdiger, Reconstitution of pigment-containing complexes from light-harvesting chlorophyll *a*/*b*-binding protein overexpressed in *Escherichia coli*, Planta 181 (1990) 204–211.
[32] E. Giuffra, D. Cugini, R. Croce, R. Bassi, Reconstitution and pigment-binding properties of recombinant CP29, Eur. J. Biochem. 238 (1996) 112–120.
[33] F. Ros, R. Bassi, H. Paulsen, Pigment-binding properties of the recombinant photosystem II subunit CP26 reconstituted in vitro, Eur. J. Biochem. 253 (1998) 653–658.
[34] A. Pagano, G. Cinque, R. Bassi, In vitro reconstitution of the recombinant photosystem II light-harvesting complex CP24 and its spectroscopic characterization, J. Biol. Chem. 273 (1998) 17154–17165.
[35] J. Standfuss, W. Kühlbrandt, The three isoforms of the light-harvesting complex II: spectroscopic features, trimer formation, and functional roles, J. Biol. Chem. 279 (2004) 36884–36891.
[36] S. Storf, S. Jansson, V.H. Schmid, Pigment binding, fluorescence properties, and oligomerization behavior of Lhca5, a novel light-harvesting protein, J. Biol. Chem. 280 (2005) 5163–5168.
[37] S. Castelletti, T. Morosinotto, B. Robert, S. Caffarri, R. Bassi, R. Croce, Recombinant Lhca2 and Lhca3 subunits of the photosystem I antenna system, Biochemistry 42 (2003) 4226–4234.
[38] V.H. Schmid, K.V. Cammarata, B.U. Bruns, G.W. Schmidt, In vitro reconstitution of the photosystem I light-harvesting complex LHCI-730: heterodimerization is

required for antenna pigment organization, Proc. Natl. Acad. Sci. U. S. A. 94 (1997) 7667–7672.
[39] W. Kühlbrandt, D.N. Wang, Y. Fujiyoshi, Atomic model of plant light-harvesting complex by electron crystallography, Nature 367 (1994) 614–621.
[40] H. Rogl, W. Kühlbrandt, Mutant trimers of light-harvesting complex II exhibit altered pigment content and spectroscopic features, Biochemistry 38 (1999) 16214–16222.
[41] R. Remelli, C. Varotto, D. Sandona, R. Croce, R. Bassi, Chlorophyll binding to monomeric light-harvesting complex. A mutation analysis of chromophore-binding residues, J. Biol. Chem. 274 (1999) 33510–33521.
[42] R. Bassi, R. Croce, D. Cugini, D. Sandona, Mutational analysis of a higher plant antenna protein provides identification of chromophores bound into multiple sites, Proc. Natl. Acad. Sci. U. S. A. 96 (1999) 10056–10061.
[43] T. Morosinotto, S. Castelletti, J. Breton, R. Bassi, R. Croce, Mutation analysis of Lhca1 antenna complex. Low energy absorption forms originate from pigment–pigment interactions, J. Biol. Chem. 277 (2002) 36253–36261.
[44] R. Croce, T. Morosinotto, J.A. Ihalainen, A. Chojnicka, J. Breton, J.P. Dekker, R. van Grondelle, R. Bassi, Origin of the 701-nm fluorescence emission of the Lhca2 subunit of higher plant photosystem I, J. Biol. Chem. 279 (2004) 48543–48549.
[45] M. Mozzo, T. Morosinotto, R. Bassi, R. Croce, Probing the structure of Lhca3 by mutation analysis, Biochim. Biophys. Acta 1757 (2006) 1607–1613.
[46] D. Corbet, T. Schweikardt, H. Paulsen, V.H. Schmid, Amino acids in the second transmembrane helix of the Lhca4 subunit are important for formation of stable heterodimeric light-harvesting complex LHCI-730, J. Mol. Biol. 370 (2007) 170–182.
[47] P.J. Booth, H. Paulsen, Assembly of light-harvesting chlorophyll *a*/*b* complex in vitro. Time-resolved fluorescence measurements, Biochemistry 35 (1996) 5103–5108.
[48] R. Horn, G. Grundmann, H. Paulsen, Consecutive binding of chlorophylls a and b during the assembly in vitro of light-harvesting chlorophyll-*a*/*b* protein (LHCIIb), J. Mol. Biol. 366 (2007) 1045–1054.
[49] V. Schmid, Light-harvesting complexes of vascular plants, Cell. Mol. Life Sci. 65 (2008) 3619–3639.
[50] S. Hobe, R. Forster, J. Klingler, H. Paulsen, N-proximal sequence motif in light-harvesting chlorophyll *a*/*b*-binding protein is essential for the trimerization of light-harvesting chlorophyll *a*/*b* complex, Biochemistry 34 (1995) 10224–10228.
[51] R.R. Green, E. Pichersky, Hypothesis for the evolution of three-helix Chl *a*/*b* and Chl *a*/*c* light-harvesting antenna proteins from two-helix and four-helix ancestors, Photosynth. Res. 39 (1994) 149–162.
[52] S. Hobe, S. Prytulla, W. Kühlbrandt, H. Paulsen, Trimerization and crystallization of reconstituted light-harvesting chlorophyll *a*/*b* complex, EMBO J. 13 (1994) 3423–3429.
[53] A.V. Ruban, M. Wentworth, A.E. Yakushevska, J. Andersson, P.J. Lee, W. Keegstra, J. P. Dekker, E.J. Boekema, S. Jansson, P. Horton, Plants lacking the main light-harvesting complex retain photosystem II macro-organization, Nature 421 (2003) 648–652.
[54] S. Jansson, H. Stefansson, U. Nyström, P. Gustafsson, P.-Å. Albertsson, Antenna protein composition of PS I and PS II in thylakoid sub-domains, Biochim. Biophys. Acta 1320 (1997) 297–309.
[55] E.J. Boekema, B. Hankamer, D. Bald, J. Kruip, J. Nield, A.F. Boonstra, J. Barber, M. Rogner, Supramolecular structure of the photosystem II complex from green plants and cyanobacteria, Proc. Natl. Acad. Sci. U. S. A. 92 (1995) 175–179.
[56] E.J. Boekema, H. van Roon, F. Calkoen, R. Bassi, J.P. Dekker, Multiple types of association of photosystem II and its light-harvesting antenna in partially solubilized photosystem II membranes, Biochemistry 38 (1999) 2233–2239.
[57] H. van Amerongen, R. van Grondelle, Understanding the energy transfer function of LHCII, the major light-harvesting complex of green plants, J. Phys. Chem. B. 105 (2001) 604–617.
[58] T. Polivka, V. Sundstrom, Ultrafast dynamics of carotenoid excited states and #x2212; from solution to natural and artificial systems, Chem. Rev. 104 (2004) 2021–2072.
[59] V.I. Novoderezhkin, M.A. Palacios, H. van Amerongen, R. van Grondelle, Excitation dynamics in the LHCII complex of higher plants: modeling based on the 2.72 Å crystal structure, J. Phys. Chem. B. 109 (2005) 10493–10504.
[60] V. Barzda, V. Gulbinas, R. Kananavicius, V. Cervinskas, H. van Amerongen, R. van Grondelle, L. Valkunas, Singlet-singlet annihilation kinetics in aggregates and trimers of LHCII, Biophys. J. 80 (2001) 2409–2421.
[61] R. van Grondelle, V.I. Novoderezhkin, Energy transfer in photosynthesis: experimental insights and quantitative models, Phys. Chem. Chem. Phys. 8 (2006) 793–807.
[62] J. Bennett, Phosphorylation of chloroplast membrane polypeptides, Nature 269 (1977) 344–346.
[63] J. Bennett, Chloroplast phosphoproteins. The protein kinase of thylakoid membranes is light-dependent, FEBS Lett. 103 (1979) 342–344.
[64] J.E. Mullet, The amino acid sequence of the polypeptide segment which regulates membrane adhesion (grana stacking) in chloroplasts, J. Biol. Chem. 258 (1983) 9941–9948.
[65] J. Bennett, K.E. Steinback, C.J. Arntzen, Chloroplast phosphoproteins: regulation of excitation energy transfer by phosphorylation of thylakoid membrane polypeptides, Proc. Natl. Acad. Sci. U. S. A. 77 (1980) 5253–5257.
[66] J.F. Allen, Protein phosphorylation in regulation of photosynthesis, Biochim. Biophys. Acta 1098 (1992) 275–335.
[67] J.F. Allen, J. Forsberg, Molecular recognition in thylakoid structure and function, Trends Plant. Sci. 6 (2001) 317–326.
[68] F.A. Wollman, State transitions reveal the dynamics and flexibility of the photosynthetic apparatus, EMBO J. 20 (2001) 3623–3630.
[69] J.F. Allen, J. Bennett, K.E. Steinback, C.J. Arntzen, Chloroplast protein phosphorylation couples plastoquinone redox state to distribution of excitation energy between photosystems, Nature 291 (1981) 25–29.
[70] S. Jansson, The light-harvesting chlorophyll *a*/*b*-binding proteins, Biochim. Biophys. Acta 1184 (1994) 1–19.
[71] S. Bellafiore, F. Barneche, G. Peltier, J.D. Rochaix, State transitions and light adaptation require chloroplast thylakoid protein kinase STN7, Nature 433 (2005) 892–895.
[72] J. Andersson, M. Wentworth, R.G. Walters, C.A. Howard, A.V. Ruban, P. Horton, S. Jansson, Absence of the Lhcb1 and Lhcb2 proteins of the light-harvesting complex of photosystem II — effects on photosynthesis, grana stacking and fitness, Plant J. 35 (2003) 350–361.
[73] I.J. Ryrie, N. Fuad, Membrane adhesion in reconstituted proteoliposomes containing the light-harvesting chlorophyll *a*/*b*-protein complex: the role of charged surface groups, Arch. Biochem. Biophys. 214 (1982) 475–488.
[74] J. Barber, Membrane surface charges and potentials in relation to photosynthesis, Biochim. Biophys. Acta 594 (1980) 253–308.
[75] A. McDonnel, L.A. Staehelin, Adhesion between liposomes mediated by the chlorophyll *a*/*b* light-harvesting complex isolated from chloroplast membranes, J. Cell. Biol. 84 (1980) 40–56.
[76] J.E. Mullet, C.J. Arntzen, Simulation of grana stacking in a model membrane system. Mediation by a purified light-harvesting pigment–protein complex from chloroplasts, Biochim. Biophys. Acta 589 (1980) 100–117.
[77] J. Li, C. Hollingshead, Formation of crystalline arrays of chlorophyll *a*/*b* — light-harvesting protein by membrane reconstitution, Biophys. J. 37 (1982) 363–370.
[78] W. Kühlbrandt, T. Thaler, E. Wehrli, The structure of membrane crystals of the light-harvesting chlorophyll *a*/*b* protein complex, J. Cell. Biol. 96 (1983) 1414–1424.
[79] M.K. Lyon, K.R. Miller, Crystallization of the light-harvesting chlorophyll *a*/*b* complex within thylakoid membranes, J. Cell. Biol. 100 (1985) 1139–1147.
[80] W. Kühlbrandt, Three-dimensional structure of the light-harvesting chlorophyll *a*/*b*–protein complex, Nature 307 (1984) 478–480.
[81] P.J. Butler, W. Kühlbrandt, Determination of the aggregate size in detergent solution of the light-harvesting chlorophyll *a*/*b*–protein complex from chloroplast membranes, Proc. Natl. Acad. Sci. U. S. A. 85 (1988) 3797–3801.
[82] D.N. Wang, W. Kühlbrandt, Three-dimensional electron diffraction of plant light-harvesting complex, Biophys. J. 61 (1992) 287–297.
[83] N. Grigorieff, T.A. Ceska, K.H. Downing, J.M. Baldwin, R. Henderson, Electron-crystallographic refinement of the structure of bacteriorhodopsin, J. Mol. Biol. 259 (1996) 393–421.
[84] R. Henderson, J.M. Baldwin, K.H. Downing, J. Lepault, F. Zemlin, Structure of purple membrane from halobacterium halobium: recording, measurement and evaluation of electron micrographs at 3.5 Å resolution, Ultramicroscopy 19 (1986) 147–178.
[85] H. Michel, D. Oesterhelt, Three-dimensional crystals of membrane proteins: bacteriorhodopsin, Proc. Natl. Acad. Sci. U. S. A. 77 (1980) 1283–1285.
[86] H. Michel, Three-dimensional crystals of a membrane protein complex. The photosynthetic reaction centre from Rhodopseudomonas viridis, J. Mol. Biol. 158 (1982) 567–572.
[87] R.M. Garavito, J.P. Rosenbusch, Three-dimensional crystals of an integral membrane protein: an initial X-ray analysis, J. Cell. Biol. 86 (1980) 327–329.
[88] W. Kühlbrandt, Three-dimensional crystals of the light-harvesting chlorophyll *a*/*b* protein complex from pea chloroplasts, J. Mol. Biol. 194 (1987) 757–762.
[89] Z. Liu, H. Yan, K. Wang, T. Kuang, J. Zhang, L. Gui, X. An, W. Chang, Crystal structure of spinach major light-harvesting complex at 2.72 Å resolution, Nature 428 (2004) 287–292.
[90] J.P. Dekker, H. van Roon, E.J. Boekema, Heptameric association of light-harvesting complex II trimers in partially solubilized photosystem II membranes, FEBS Lett. 449 (1999) 211–214.
[91] J. Standfuss, A.C. Terwisscha van Scheltinga, M. Lamborghini, W. Kühlbrandt, Mechanisms of photoprotection and nonphotochemical quenching in pea light-harvesting complex at 2.5 Å resolution, EMBO J. 24 (2005) 919–928.
[92] H. Michel, Crystallization of membrane proteins, Trends Biochem. Sci. 8 (1983) 56–59.
[93] W. Kühlbrandt, D.N. Wang, Three-dimensional structure of plant light-harvesting complex determined by electron crystallography, Nature 350 (1991) 130–134.
[94] N.E. Hoffman, E. Pichersky, V.S. Malik, C. Castresana, K. Ko, S.C. Darr, A.R. Cashmore, A cDNA clone encoding a photosystem I protein with homology to photosystem II chlorophyll *a*/*b*-binding polypeptides, Proc. Natl. Acad. Sci. U. S. A. 84 (1987) 8844–8848.
[95] K. Murata, K. Mitsuoka, T. Hirai, T. Walz, P. Agre, J.B. Heymann, A. Engel, Y. Fujiyoshi, Structural determinants of water permeation through aquaporin-1, Nature 407 (2000) 599–605.
[96] A. Yamashita, S.K. Singh, T. Kawate, Y. Jin, E. Gouaux, Crystal structure of a bacterial homologue of Na+/Cl-dependent neurotransmitter transporters, Nature 437 (2005) 215–223.
[97] S. Faham, A. Watanabe, G.M. Besserer, D. Cascio, A. Specht, B.A. Hirayama, E.M. Wright, J. Abramson, The crystal structure of a sodium galactose transporter reveals mechanistic insights into Na+/sugar symport, Science 321 (2008) 810–814.
[98] B.R. Green, W. Kühlbrandt, Sequence conservation of light-harvesting and stress-response proteins in relation to the three-dimensional molecular structure of LHCII, Photosynth. Res. 44 (1995) 139–148.

[99] A. Kuttkat, A. Hartmann, S. Hobe, H. Paulsen, The C-terminal domain of light-harvesting chlorophyll-*a*/*b*-binding protein is involved in the stabilisation of trimeric light-harvesting complex, Eur. J. Biochem. 242 (1996) 288–292.
[100] C. Tanford, Contribution of hydrophobic interactions to the stability of the globular conformation of proteins, J. Am. Chem. Soc. 84 (1962) 4240–4247.
[101] D.A. Day, I.J. Ryrie, N. Fuad, Investigations of the role of the main light-harvesting chlorophyll–protein complex in thylakoid membranes. Reconstitution of depleted membranes from intermittent-light-grown plants with the isolated complex, J. Cell. Biol. 98 (1984) 163–172.
[102] R. Croce, G. Canino, F. Ros, R. Bassi, Chromophore organization in the higher-plant photosystem II antenna protein CP26, Biochemistry 41 (2002) 7334–7343.
[103] H. Paulsen, B. Finkenzeller, N. Kuhlein, Pigments induce folding of light-harvesting chlorophyll *a*/*b*-binding protein, Eur. J. Biochem. 215 (1993) 809–816.
[104] A. Strand, K. Kvernberg, M.K.A., S. Liaaen-Jensen, Geometrical E/Z isomers of (6R)- and (6S)-neoxanthin and biological implications, Biochem. Syst. Ecol. 28 (2000) 443–455.
[105] S. Takaichi, M. Mirauro, Distribution and geometric isomerism of neoxanthin in oxygenic phototrophs: 9′-*cis*, a sole molecular form, Plant. Cell. Physiol. 39 (1998) 968–977.
[106] L. Dall'Osto, S. Cazzaniga, H. North, A. Marion-Poll, R. Bassi, The *Arabidopsis* aba4-1 mutant reveals a specific function for neoxanthin in protection against photooxidative stress, Plant. Cell. 19 (2007) 1048–1064.
[107] A.V. Ruban, P.J. Lee, M. Wentworth, A.J. Young, P. Horton, Determination of the stoichiometry and strength of binding of xanthophylls to the photosystem II light harvesting complexes, J. Biol. Chem. 274 (1999) 10458–10465.
[108] R.J. Porra, W.A. Thompson, P.E. Kriedemann, Determination of accurate extinction coefficients and simultaneous equations for assaying chlorophylls a and b extracted with four different solvents: verification of the concentration of chlorophyll standards by atomic absorption spectroscopy, Biochim. Biophys. Acta 975 (1989) 384–394.
[109] T. Barros, A. Royant, J. Standfuss, A. Dreuw, W. Kuhlbrandt, Crystal structure of plant light-harvesting complex shows the active, energy-transmitting state, EMBO J. 28 (2009) 298–306.
[110] H. Yan, P. Zhang, C. Wang, Z. Liu, W. Chang, Two lutein molecules in LHCII have different conformations and functions: insights into the molecular mechanism of thermal dissipation in plants, Biochem. Biophys. Res. Commun. 355 (2007) 457–463.
[111] H.Y. Yamamoto, T.O.M. Nakayama, C.O. Chichester, Studies on the light and dark interconversions of leaf xanthophylls, Arch. Biochem. Biophys. 97 (1962) 168–173.
[112] H.Y. Yamamoto, Xanthophyll Cycles, Methods in Enzymology, Vol. 110, Academic Press, 1985, pp. 303–312.
[113] A. Trémolières, J.P. Dubacq, F. Ambard-Bretteville, R. RÈmy, Lipid composition of chlorophyl–protein complexes: specific enrichment in trans-hexadecenoic acid of an oligomeric form of light-harvesting chlorophyll *a*/*b* protein, FEBS Lett. 130 (1981) 27–31.
[114] S. Nussberger, K. Dorr, D.N. Wang, W. Kuhlbrandt, Lipid–protein interactions in crystals of plant light-harvesting complex, J. Mol. Biol. 234 (1993) 347–356.
[115] A.A. Pascal, Z. Liu, K. Broess, B. van Oort, H. van Amerongen, C. Wang, P. Horton, B. Robert, W. Chang, A. Ruban, Molecular basis of photoprotection and control of photosynthetic light-harvesting, Nature 436 (2005) 134–137.
[116] A.V. Ruban, P. Horton, B. Robert, Resonance Raman spectroscopy of the photosystem II light-harvesting complex of green plants: a comparison of trimeric and aggregated states, Biochemistry 34 (1995) 2333–2337.
[117] A.V. Ruban, R. Berera, C. Ilioaia, I.H. van Stokkum, J.T. Kennis, A.A. Pascal, H. van Amerongen, B. Robert, P. Horton, R. van Grondelle, Identification of a mechanism of photoprotective energy dissipation in higher plants, Nature 450 (2007) 575–578.
[118] A. Amunts, O. Drory, N. Nelson, The structure of a plant photosystem I supercomplex at 3.4 Å resolution, Nature 447 (2007) 58–63.
[119] D. Das, S.S. Krishna, D. McMullan, M.D. Miller, Q. Xu, P. Abdubek, C. Acosta, T. Astakhova, H.L. Axelrod, P. Burra, D. Carlton, H.-J. Chiu, T. Clayton, M.C. Deller, L. Duan, Y. Elias, M.-A. Elsliger, D. Ernst, J. Feuerhelm, A. Grzechnik, S.K. Grzechnik, J. Hale, G.W. Han, L. Jaroszewski, K.K. Jin, H.E. Klock, M.W. Knuth, P. Kozbial, A. Kumar, D. Marciano, A.T. Morse, K.D. Murphy, E. Nigoghossian, L. Okach, S. Oommachen, J. Paulsen, R. Reyes, C.L. Rife, N. Sefcovic, H. Tien, C.B. Trame, C.V. Trout, H.V.D. Bedem, D. Weekes, A. White, K.O. Hodgson, J. Wooley, A.M. Deacon, A. Godzik, S.A. Lesley, I.A. Wilson, Crystal structure of the Fic (Filamentation induced by cAMP) family protein SO4266 (gi|24375750) from *Shewanella oneidensis* MR-1 at 1.6 Å resolution, Proteins: Struct. Funct. Bioinf. 75 (2009) 264–271.
[120] P.K. Haripal, H.K. Raval, M.K. Raval, R.M. Rawal, B. Biswal, U.C. Biswal, Three-dimensional model of zeaxanthin binding PsbS protein associated with nonphotochemical quenching of excess quanta of light energy absorbed by the photosynthetic apparatus, J. Mol. Model. 12 (2006) 847–853.
[121] P. Müller, X.-P. Li, K.K. Niyogi, Non-photochemical quenching. A response to excess light energy, Plant Physiol. 125 (2001) 1558–1566.
[122] C. Külheim, J. Ågren, S. Jansson, Rapid regulation of light harvesting and plant fitness in the field. Science 297 (2002) 91–93.
[123] A. Ruban, P. Horton, Spectroscopy of non-photochemical and photochemical quenching of chlorophyll fluorescence in leaves; evidence for a role of the light harvesting complex of Photosystem II in the regulation of energy dissipation, Photosynth. Res. 40 (1994) 181–190.
[124] J.P. Ide, D.R. Klug, W. Kühlbrandt, L.B. Giorgi, G. Porter, The state of detergent solubilized light-harvesting chlorophyll-*a*/*b* protein complex as monitored by picosecond time-resolved fluorescence and circular-dichroism, Biochim. Biophys. Acta 893 (1987) 349–364.
[125] C.W. Mullineaux, A.A. Pascal, P. Horton, A.R. Holzwarth, Excitation-energy quenching in aggregates of the LHC II chlorophyll–protein complex: a time-resolved fluorescence study, Biochim. Biophys. Acta 1141 (1993) 23–28.
[126] A.V. Ruban, P. Horton, Mechanism of [Delta]pH-dependent dissipation of absorbed excitation energy by photosynthetic membranes. I. Spectroscopic analysis of isolated light-harvesting complexes, Biochim. Biophys. Acta 1102 (1992) 30–38.
[127] S. Vasil'ev, K.D. Irrgang, T. Schrotter, A. Bergmann, H.J. Eichler, G. Renger, Quenching of chlorophyll a fluorescence in the aggregates of LHCII: steady state fluorescence and picosecond relaxation kinetics, Biochemistry 36 (1997) 7503–7512.
[128] V. Barzda, C.J. de Grauw, J. Vroom, F.J. Kleima, R. van Grondelle, H. van Amerongen, H.C. Gerritsen, Fluorescence lifetime heterogeneity in aggregates of LHCII revealed by time-resolved microscopy, Biophys. J. 81 (2001) 538–546.
[129] H. Kirchhoff, H.J. Hinz, J. Rosgen, Aggregation and fluorescence quenching of chlorophyll a of the light-harvesting complex II from spinach in vitro, Biochim. Biophys. Acta 1606 (2003) 105–116.
[130] P.H. Lambrev, Z. Varkonyi, S. Krumova, L. Kovacs, Y. Miloslavina, A.R. Holzwarth, G. Garab, Importance of trimer–trimer interactions for the native state of the plant light-harvesting complex II, Biochim. Biophys. Acta 1767 (2007) 847–853.
[131] B. van Oort, A. van Hoek, A.V. Ruban, H. van Amerongen, Aggregation of light-harvesting complex II leads to formation of efficient excitation energy traps in monomeric and trimeric complexes, FEBS Lett. 581 (2007) 3528–3532.
[132] A.V. Ruban, J.P. Dekker, P. Horton, R.V.A.N. Grondelle, Temperature dependence of chlorophyll fluorescence from light-harvesting complex II of higher plants, Photochem. Photobiol. 61 (1995) 216–221.
[133] A.M. Gilmore, T.L. Hazlett, Govindjee, xanthophyll cycle-dependent quenching of photosystem ii chlorophyll a fluorescence: formation of a quenching complex with a short fluorescence lifetime, Proc. Natl. Acad. Sci. U. S. A. 92 (1995) 2273–2277.
[134] A.V. Ruban, D. Rees, G.D. Noctor, A. Young, P. Horton, Long-wavelength chlorophyll species are associated with amplification of high-energy-state excitation quenching in higher plants, Biochim. Biophys. Acta 1059 (1991) 355–360.
[135] P. Horton, A.V. Ruban, D. Rees, A.A. Pascal, G. Noctor, A.J. Young, Control of the light-harvesting function of chloroplast membranes by aggregation of the LHCII chlorophyll–protein complex, FEBS Lett. 292 (1991) 1–4.
[136] P. Horton, M. Wentworth, A. Ruban, Control of the light harvesting function of chloroplast membranes: the LHCII-aggregation model for non-photochemical quenching, FEBS Lett. 579 (2005) 4201–4206.
[137] Y. Miloslavina, A. Wehner, P.H. Lambrev, E. Wientjes, M. Reus, G. Garab, R. Croce, A.R. Holzwarth, Far-red fluorescence: a direct spectroscopic marker for LHCII oligomer formation in non-photochemical quenching, FEBS Lett. 582 (2008) 3625–3631.
[138] P. Jahns, D. Latowski, K. Strzalka, Mechanism and regulation of the violaxanthin cycle: the role of antenna proteins and membrane lipids, Biochim. Biophys. Acta 1787 (2009) 3–14.
[139] M. Wentworth, A.V. Ruban, P. Horton, Chlorophyll fluorescence quenching in isolated light harvesting complexes induced by zeaxanthin, FEBS Lett. 471 (2000) 71–74.
[140] T.J. Avenson, T.K. Ahn, D. Zigmantas, K.K. Niyogi, Z. Li, M. Ballottari, R. Bassi, G.R. Fleming, Zeaxanthin radical cation formation in minor light-harvesting complexes of higher plant antenna, J. Biol. Chem. 283 (2008) 3550–3558.
[141] S. Amarie, J. Standfuss, T. Barros, W. Kühlbrandt, A. Dreuw, J. Wachtveitl, Carotenoid radical cations as a probe for the molecular mechanism of nonphotochemical quenching in oxygenic photosynthesis, J. Phys. Chem. B. 111 (2007) 3481–3487.
[142] S. Bode, C.C. Quentmeier, P.-N. Liao, T. Barros, P.J. Walla, Xanthophyll-cycle dependence of the energy transfer between carotenoid dark states and chlorophylls in NPQ mutants of living plants and in LHC II, Chem. Phys. Lett. 450 (2008) 379–385.
[143] A. Dreuw, M. Wormit, Simple replacement of violaxanthin by zeaxanthin in LHC-II does not cause chlorophyll fluorescence quenching, J. Inorg. Biochem. 102 (2008) 458–465.
[144] B. Demmig, K. Winter, A. Kruger, F.C. Czygan, Photoinhibition and zeaxanthin formation in intact leaves: a possible role of the xanthophyll cycle in the dissipation of excess light energy, Plant. Physiol. 84 (1987) 218–224.
[145] T.J. Avenson, T.K. Ahn, K.K. Niyogi, M. Ballottari, R. Bassi, G.R. Fleming, Lutein can act as a switchable charge-transfer quencher in the CP26 light-harvesting complex, J. Biol. Chem. (2008).
[146] M.L. Perez-Bueno, M.P. Johnson, A. Zia, A.V. Ruban, P. Horton, The Lhcb protein and xanthophyll composition of the light harvesting antenna controls the DeltapH-dependency of non-photochemical quenching in *Arabidopsis thaliana*, FEBS Lett. 582 (2008) 1477–1482.
[147] L. Dall'Osto, S. Caffarri, R. Bassi, A mechanism of nonphotochemical energy dissipation, independent from PsbS, revealed by a conformational change in the antenna protein CP26, Plant. Cell. 17 (2005) 1217–1232.
[148] S. Crouchman, A. Ruban, P. Horton, PsbS enhances nonphotochemical fluorescence quenching in the absence of zeaxanthin, FEBS Lett. 580 (2006) 2053–2058.
[149] P. Horton, A.V. Ruban, M. Wentworth, Allosteric regulation of the light-harvesting system of photosystem II, Philos. Trans. R. Soc. Lond. B. Biol. Sci. 355 (2000) 1361–1370.
[150] H.A. Frank, A. Cua, V. Chynwat, A. Young, D. Gosztola, M.R. Wasielewski, Photophysics of the carotenoids associated with the xanthophyll cycle in photosynthesis, Photosynth. Res. 41 (1994) 389–395.

[151] A. Dreuw, G.R. Fleming, M. Head-Gordon, Chlorophyll fluorescence quenching by xanthophylls, Phys. Chem. Chem. Phys. 5 (2003) 3247–3256.
[152] N.E. Holt, D. Zigmantas, L. Valkunas, X.P. Li, K.K. Niyogi, G.R. Fleming, Carotenoid cation formation and the regulation of photosynthetic light harvesting, Science 307 (2005) 433–436.
[153] T.K. Ahn, T.J. Avenson, M. Ballottari, Y.-C. Cheng, K.K. Niyogi, R. Bassi, G.R. Fleming, Architecture of a charge-transfer state regulating light harvesting in a plant antenna protein, Science 320 (2008) 794–797.
[154] K.K. Niyogi, A.R. Grossman, O. Bjorkman, *Arabidopsis* mutants define a central role for the xanthophyll cycle in the regulation of photosynthetic energy conversion, Plant Cell. 10 (1998) 1121–1134.
[155] G.S. Beddard, G. Porter, Concentration quenching in chlorophyll, Nature 260 (1976) 366–367.
[156] I. Moya, M. Silvestri, O. Vallon, G. Cinque, R. Bassi, Time-resolved fluorescence analysis of the photosystem II antenna proteins in detergent micelles and liposomes, Biochemistry 40 (2001) 12552–12561.
[157] A.M. Gilmore, H.Y. Yamamoto, Dark induction of zeaxanthin-dependent nonphotochemical fluorenscence quenching mediated by ATP, Proc. Natl. Acad. Sci. U. S. A. 89 (1992) 1899–1903.
[158] B. van Oort, A. van Hoek, A.V. Ruban, H. van Amerongen, Equilibrium between quenched and nonquenched conformations of the major plant light-harvesting complex studied with high-pressure time-resolved fluorescence, J. Phys. Chem. B. 111 (2007) 7631–7637.
[159] C. Ilioaia, M.P. Johnson, P. Horton, A.V. Ruban, Induction of efficient energy dissipation in the isolated light-harvesting complex of photosystem II in the absence of protein aggregation, J. Biol. Chem. 283 (2008) 29505–29512.
[160] T. Barros, A. Royant, J. Standfuss, A. Dreuw, W. Kuhlbrandt, Crystal structure of plant light-harvesting complex shows the active, energy-transmitting state, EMBO J. 28 (2009) 298–306.
[161] X.P. Li, O. Bjorkman, C. Shih, A.R. Grossman, M. Rosenquist, S. Jansson, K.K. Niyogi, A pigment-binding protein essential for regulation of photosynthetic light harvesting, Nature 403 (2000) 391–395.
[162] C. Funk, I. Adamska, B.R. Green, B. Andersson, G. Renger, The nuclear-encoded chlorophyll-binding photosystem II-S protein is stable in the absence of pigments, J. Biol. Chem. 270 (1995) 30141–30147.
[163] M. Aspinall-O'Dea, M. Wentworth, A. Pascal, B. Robert, A. Ruban, P. Horton, In vitro reconstitution of the activated zeaxanthin state associated with energy dissipation in plants, Proc. Natl. Acad. Sci. U. S. A. 99 (2002) 16331–16335.
[164] G. Bonente, B.D. Howes, S. Caffarri, G. Smulevich, R. Bassi, Interactions between the photosystem II subunit PsbS and xanthophylls studied in vivo and in vitro, J. Biol. Chem. 283 (2008) 8434–8445.
[165] E. Bergantino, A. Segalla, A. Brunetta, E. Teardo, F. Rigoni, G.M. Giacometti, I. Szabo, Light- and pH-dependent structural changes in the PsbS subunit of photosystem II, Proc. Natl. Acad. Sci. U. S. A. 100 (2003) 15265–15270.
[166] X.-P. Li, A. Phippard, J. Pasari, K.K. Niyogi, Structure–function analysis of photosystem II subunit S (PsbS) *in vivo*, Funct. Plant Biol. 29 (2002) 1131–1139.
[167] E. Teardo, P.P. de Laureto, E. Bergantino, F. Dalla Vecchia, F. Rigoni, I. Szabo, G.M. Giacometti, Evidences for interaction of PsbS with photosynthetic complexes in maize thylakoids, Biochim. Biophys. Acta 1767 (2007) 703–711.
[168] I. Szabo, E. Bergantino, G.M. Giacometti, Light and oxygenic photosynthesis: energy dissipation as a protection mechanism against photo-oxidation, EMBO Rep. 6 (2005) 629–634.
[169] J. Deisenhofer, O. Epp, K. Miki, R. Huber, H. Michel, Structure of the protein subunits in the photosynthetic reaction centre of Rhodopseudomonas viridis at 3 Å resolution, Nature 318 (1985) 618–624.
[170] R. Henderson, J.M. Baldwin, T.A. Ceska, F. Zemlin, E. Beckmann, K.H. Downing, Model for the structure of bacteriorhodopsin based on high-resolution electron cryo-microscopy, J. Mol. Biol. 213 (1990) 899–929.
[171] M.S. Weiss, T. Wacker, J. Weckesser, W. Welte, G.E. Schulz, The three-dimensional structure of porin from Rhodobacter capsulatus at 3 Å resolution, FEBS Lett. 267 (1990) 268–272.
[172] S.W. Cowan, T. Schirmer, G. Rummel, M. Steiert, R. Ghosh, R.A. Pauptit, J.N. Jansonius, J.P. Rosenbusch, Crystal structures explain functional properties of two *E. coli* porins, Nature 358 (1992) 727–733.
[173] R.C. Edgar, MUSCLE: multiple sequence alignment with high accuracy and high throughput, Nucl. Acids Res. 32 (2004) 1792–1797.
[174] M. Crimi, D. Dorra, C.S. Bosinger, E. Giuffra, A.R. Holzwarth, R. Bassi, Time-resolved fluorescence analysis of the recombinant photosystem II antenna complex CP29. Effects of zeaxanthin, pH and phosphorylation, Eur. J. Biochem. 268 (2001) 260–267.